



Shahrood University of  
Technology



Iranian Society of  
Mining Engineering  
(IRSE)

# Development of an Integrated Framework for Optimizing Mine Drainage Systems: Utilizing Numerical Modeling, Decision-Making and Machine Learning Applications

Seyyedeh Golaleh Hosseini\*, Kourosch Shahriar and Mohammadamin Karbala

Mining Engineering, Mining, Amirkabir University of Technology (Tehran Polytechnic), Tehran, Iran

## Article Info

Received 5 January 2025

Received in Revised form 13 July 2025

Accepted 2 August 2025

Published online 2 August 2025

DOI: [10.22044/jme.2025.15562.2982](https://doi.org/10.22044/jme.2025.15562.2982)

## Keywords

Mine Drainage Management

Numerical Modeling

Machine Learning

Decision-Making Frameworks

Sustainable Water Treatment

## Abstract

Mine drainage remains a critical challenge in ensuring the safety and sustainability of mining operations, as it is often complicated by complex subsurface flow behaviors and mechanical stress interactions. This study proposes an integrated three-phase framework for analyzing and optimizing drainage systems at the Angouran lead–zinc mine. In the first phase, the hydro-mechanical behavior of the rock mass was simulated using UDEC software, demonstrating that increased normal stress reduces fracture aperture and permeability. The simulated pore pressure ( $4.5 \times 10^5$  Pa) closely matched the field measurements ( $4.4 \times 10^5$  Pa), with only a 2.2% deviation. In the second phase, a multi-criteria decision-making approach using the Analytic Hierarchy Process (AHP) and input from 32 domain experts identified Q4 (very high quality) and Q2 (medium quality) indicators as the most influential criteria. In the third phase, three machine learning models—linear regression, polynomial regression, and artificial neural networks (ANNs)—were trained on piezometric data to predict water discharge. The ANN model outperformed the other models, achieving an  $R^2$  of 0.94 and RMSE of 0.18, effectively capturing the nonlinear dynamics of groundwater flow within the mine. The findings highlight that the integration of numerical modeling, expert-based decision analysis, and AI-driven prediction provides a robust and innovative approach for designing and managing mine dewatering systems, with potential applicability to other complex hydrogeological environments.

## 1. Introduction

Mine drainage constitutes one of the most significant environmental and technical challenges faced by modern mining operations. Contaminated water—laden with heavy metals, acids, and toxic compounds—threatens freshwater resources, public health, and ecological balance. Acid mine drainage (AMD), resulting from the oxidation of sulfide minerals exposed during mining activities, is a major source of water pollution in metallic mines. Field studies from sites such as the Sukinda Chromite Mine in India, along with reports of arsenic contamination in groundwater near mining

regions highlight the widespread and urgent nature of this global issue.

Conventional mine drainage management methods, including active systems (e.g., chemical precipitation) and passive systems (e.g., constructed wetlands), have demonstrated varying degrees of effectiveness. However, these methods frequently encounter significant limitations, such as high operational costs, sensitivity to environmental conditions, and limited adaptability to the dynamic nature of underground mining environments. In particular, the complex hydro-



Corresponding author: Email Adresse (S.G. Hosseini)

mechanical behavior of fractured rock masses, combined with nonlinear changes in permeability under stress, presents a multidimensional challenge for the accurate prediction and control of water flow in mines.

To address these challenges, this study proposes an innovative, integrated framework for smart drainage management in mining environments. The framework integrates three complementary domains: (1) advanced numerical modeling of hydro-mechanical behavior using the Universal Distinct Element Code (UDEC), (2) expert-based multi-criteria decision analysis through the Analytic Hierarchy Process (AHP), and (3) application of artificial intelligence techniques, including regression models and artificial neural networks, for discharge prediction using real piezometric data.

As part of future directions, this study proposes the integration of Internet of Things (IoT) sensors for continuous monitoring, and the use of renewable energy-based water treatment systems in remote mining environments. While not implemented in the current phases, these technologies hold significant potential for improving real-time data acquisition, reducing operational costs, and enhancing environmental sustainability. Their incorporation into future smart drainage frameworks could offer adaptive, efficient, and scalable solutions to support long-term water resource management in mining operations.

## 2. Literature Review

To establish a comprehensive decision-making framework for mine drainage management, a thorough review of previous studies across various domains—including traditional methods, numerical modeling, multi-criteria decision-making, and artificial intelligence—is essential. The selected literature in this section is categorized into four main thematic areas:

1. **Traditional active and passive drainage control methods**,
2. **Hydro-mechanical numerical modeling approaches**, such as UDEC,
3. **Data-driven techniques and machine learning models** for discharge prediction,
4. **Integrated decision-making frameworks** involving tools like GIS, AHP, and fuzzy logic.

Despite extensive efforts in the literature, most studies have addressed only one aspect of the drainage problem in isolation. For example, numerical models often lack integration with real-time monitoring or dynamic adaptability, while machine learning approaches are rarely combined with physical modeling or expert-based analysis. Additionally, traditional and nature-based treatment methods suffer from limitations in scalability and long-term performance.

Table 1 presents a structured comparative overview of key studies, highlighting their methods, objectives, contributions, and existing research gaps. This analysis demonstrates that the present study uniquely addresses these shortcomings by integrating numerical modeling, expert-based decision analysis, and machine learning techniques into a unified and innovative framework for smart mine drainage management.

Table 2 presents several examples of various mine dewatering methods. The choice of an appropriate method is influenced by several factors, including the mine's geology, the depth of the water table, the volume of water to be extracted, and the specific requirements of the mining operation. Consulting with experts and engineers is essential to determine the most suitable dewatering method for a given mine.

## 3. Methodology

This methodology begins with numerical modeling, which serves as the foundation for this study by simulating hydraulic conditions such as water flow, permeability, and leakage in rock mass environments. Software such as Itasca and UDEC were used for these simulations. Although other tools like COMSOL and MATLAB are capable of modeling such conditions, the primary focus in this study was on UDEC. These simulations capture continuous, porous, and dual-porosity environments, providing essential input data for subsequent stages of the research.

In the next phase, decision-making models are developed by integrating expert evaluations. Through structured surveys, experts identify and prioritize influential factors using linguistic variables (e.g., very high, high, medium, low). These factors are normalized and weighted, leading to the construction of a decision matrix that facilitates the comparison of various strategies, thereby enabling optimal resource allocation and effective risk management.

**Table 1. Comparative Summary of Key Studies on Mine Drainage Management: Methods, Contributions, and Research Gaps**

Reference	Method / Tool	Objective	Key Contribution	Identified Gap
RoyChowdhury et al. (2015) [1]	Active Treatment Methods	Neutralize acidity, remove heavy metals	Overview of chemical precipitation & oxidation methods	High cost, operational complexity
Skousen et al. (2017) [2]	Passive Systems	Long-term drainage control	Use of wetlands, limestone drains, bioreactors	Limited adaptability, slow performance
Saha et al. (2016) [3]	Phytoremediation	Remove Cr(VI) using water hyacinth	Nature-based solution for heavy metal removal	Dependent on plant performance, low scalability
Hanak & Lund (2012) [4]	Policy + Hydrology	Climate-resilient water planning	Integration of planning under uncertainty	Lacks technical modeling tools
Jing & Stephansson (2007) [5]	UDEC Modeling	Hydro-mechanical behavior	Simulated stress-flow interaction in fractured rocks	Not linked with AI or real-time data
Jodeiri Shokri et al. (2020) [6]	Gene Expression Programming (GEP)	Predict AMD potential	Development AI model for tailing risk	Limited to tailings: lacks hydro-mechanical linkage
Ahmed et al. (2021) [7]	Machine Learning	Predict groundwater flow	ML model for discharge forecasting	Ignores mechanical rock behavior
He et al. (2022) [8]	Smart Sensors (IoT)	Water quality monitoring	Continuous field monitoring using sensors	Missing integration with drainage modeling
Babaeian et al. (2023) [9]	AI, Stats, MCDM	Predict flyrock distance	Hybrid model combining expert input and AI	Not applied to water drainage or hydrology
Karampatsis et al. (2019) [10]	Sustainability-Based AMD Treatment	Eco-friendly methods for AMD	Strategies for sustainable remediation	Lack of system-level implementation models
Mandal et al. (2016) [11]	MCDM + GIS	Delineating groundwater potential zones	Integrated spatial and decision analysis	Not tailored for dynamic mine drainage systems
Shabani et al. (2017) [12]	Experimental (Nano-Remediation)	Evaluate AMD interaction with magnetic nanominerals	Demonstrated the potential of magnetic nanomaterials in AMD treatment	Lacks large-scale application and system integration
Mallick et al. (2018) [13]	Fuzzy-AHP + GIS	Landslide risk & drainage analysis	Fuzzy decision-making in complex terrain	Focused on surface risks, not subsurface drainage
Pouresmaeili et al. (2024) [14]	MCDM review	Evaluate and compare MCDM methods for sustainable mining	Comprehensive review of MCDM approaches in mining, with focus on sustainability	Lack of integration with real-time and dynamic drainage modeling
This Study	UDEC + AHP + AI	Smart mine drainage framework	Combines mechanistic modeling, expert input & AI	Fills the methodological gap by linking physical, expert, and data-driven layers

In the artificial intelligence phase, data from the Angouran Mine's piezometric measurements are used to develop predictive models. These data are particularly useful for analyzing the relationships between hydraulic variables and various environmental features of the mine. A linear regression model is utilized to simulate and predict parameters such as flow rate and hydraulic conditions under different scenarios at the Angouran Mine. This model analyzes the relationship between water pressure and the factors affecting mine drainage, thus improving prediction accuracy and optimizing decision-making. The model is continuously updated, adapting to changes in hydraulic conditions, which ultimately enhances the efficiency of drainage strategies.

### 3.1. Numerical Modeling

Numerical modeling is employed to assess permeability and evaluate fluid flow through a rock

mass. A rock formation can be classified as either permeable or impermeable. These models can incorporate the characteristics of discontinuities, including their correlations and distributions, to reduce errors. Key characteristics considered include the size, apertures, positions, and orientations of discontinuities. Numerous studies have utilized numerical methods to assess the permeability of rock masses. Advanced models typically use the finite element method (FEM) and the finite difference method (FDM), treating the rock mass as a continuous entity while defining the general properties of both the rock and its discontinuities within this framework. In contrast, discrete models often rely on methods such as the distinct element method (DEM) and discontinuous deformation analysis (DDA), wherein the rock mass is represented as discrete elements. Additionally, discrete particle-based models employ the particle flow method (PFM), which analyzes the movement of particles and blocks by solving Newton's second law.

Numerical techniques are often implemented using software such as 3DEC, UDEC, Comsol, and Hydrogeosphere. One notable example is UDEC (Universal Distinct Element Code), which offers a two-dimensional assessment of permeability and allows for the extrapolation of results into three dimensions. UDEC is based on the discrete element method and block theory developed by Goodman and Shi (1985) [14], which has become a cornerstone in simulating jointed rock mass behavior in mining and geotechnical engineering. UDEC models the rock as a collection of impermeable blocks separated by discontinuities, such as faults and joints. This software is capable of simulating hydromechanical coupling behaviors and ensures the conservation of momentum and energy in its dynamic simulations, while fluid flow calculations are derived from Darcy's law. Typically, calculations using codes like UDEC are confined to detailed studies at small scales (less than 50 meters), two-dimensional fracture networks, or random representations of larger models. UDEC can be employed to simulate the impact of stress on hydraulic conductivity and define the representative elementary volume (REV) in rock mass structures.

New software, such as FLAC (Fast Lagrangian Analysis of Continua), is now being used to calculate groundwater flow in underground

excavations and to simulate the hydrogeomechanical behavior of rock masses.

The numerical simulation of the hydromechanical behavior of a rock mass involves four key stages:

1. **Modeling the elastic/elastoplastic response** of the rock mass to applied stress.
2. **Evaluating the nonlinear response** of fractures to stress.
3. **Assessing the anticipated extent of fracturing** under stress conditions.
4. **Coupling the geomechanical model** with hydrological solvers.

Additionally, nine parameters can significantly influence the permeability of a discrete fracture network (DFN): fracture length distribution, opening distribution, surface roughness of fractures, fracture connectivity, number of intersections, hydraulic gradient, boundary stress, anisotropy, and scale. Stress is the primary parameter considered in the study of the hydromechanical behavior of a rock mass, as determining permeability at depth is essential. As depth increases, in-situ stress also rises. Research on stress has investigated natural, shear, and normal stresses, all of which must account for pore pressure and its influence on effective stress [15].

**Table 2. Examples of different types of mine dewatering methods**

mine dewatering methods	Definition
<b>Mine dewatering</b>	Mine dewatering is an essential process in mining operations, aimed at removing water from underground mines to facilitate safe and efficient extraction activities. Various mine dewatering methods can be utilized, tailored to the specific conditions and requirements of each mining site. This discussion will focus on some of the most commonly employed dewatering techniques.
<b>Open Pit Dewatering</b>	This method is used in open-pit mining when the water table lies above the mining level. It utilizes pumps to extract water from the pit and directs it to an appropriate discharge location. Open-pit dewatering can be accomplished through various techniques, including wellpoints, sumps, and perimeter ditches.
<b>Deep Well Dewatering</b>	Deep well dewatering is used when the water table lies below the mining level. This method involves drilling deep wells into the ground and installing pumps to extract water from the aquifer. The extracted water is then discharged to an appropriate location. This approach is effective in controlling groundwater inflow into the mine.
<b>Horizontal Drainage</b>	Horizontal drainage is a technique used to intercept and redirect groundwater flow away from the mining area. This method involves the installation of horizontal drains or galleries that collect and transport water to a designated discharge point. It is commonly utilized in underground mining to effectively control water inflow.
<b>In-Pit Pumping</b>	In-pit pumping is a technique used in open-pit mining to remove water from the pit. This method involves installing pumps at the bottom of the pit to extract water and discharge it to an appropriate location. In-pit pumping is effective in managing water accumulation within the pit, thereby ensuring safe working conditions.
<b>Submersible Pumping</b>	Submersible pumping is a flexible technique applicable in both open-pit and underground mining operations. This method utilizes submersible pumps, which are designed to be submerged in water for effective extraction. These pumps can manage high volumes of water and are relatively easy to install and operate across different mining environments.
<b>Vacuum Assisted WellPoint System</b>	This method is commonly employed in shallow open-pit mines or construction sites where the water table is high. It involves installing wellpoints around the excavation area, which are connected to a vacuum pump. The vacuum created by the pump lowers the water table, facilitating dewatering of the surrounding area.
<b>Grouting</b>	Grouting is a technique used for controlling water inflow in underground mining operations. This method involves injecting grout materials into the surrounding rock mass to seal water-bearing fractures and diminish water flow. Grouting can be accomplished using cementitious grouts, chemical grouts, or a combination of both.

In addition to numerical experiments, laboratory studies on single joint fractures have demonstrated that factors such as typical closure and shear dilation, the presence of fracture fill materials, and effective flow areas can significantly influence fracture permeability. Some research has explored the impact of thermal stress on permeability as well. Sensitivity analyses through numerical modeling indicate that as normal stress increases, the flow rate (permeability) decreases [16]. Moreover, when stress is applied and intensified, the likelihood of brittle failure and crack propagation increases, particularly in inactive hydraulic fractures. This can lead to a significant rise in the permeability of fractured rocks as new fractures form and connections are enhanced.

After applying existing analytical models to evaluate inflow rates into underground excavations

for more precise assessments, numerical models are utilized to estimate groundwater inflow rates and analyze how these rates vary with depth. Depth is a critical parameter for evaluating underground excavations, as it plays a significant role in estimating the permeability of the rock mass and the associated inflow rates. Generally, both numerical and analytical modeling, along with empirical formulas for permeability changes with depth, produce similar trends. According to the cube law, joint opening exerts the greatest influence on the hydrological behavior of a rock mass, affecting fracture openings, permeability, and flow rates. Given that hydraulic opening is a key input for numerical models and mechanical opening is the only measurable parameter through physical investigations, various studies have explored the relationship between mechanical and hydraulic openings (table 3).

**Table 3. Relationship between mechanical and hydraulic openings**

Author(s)	Equation	Explanation of Symbols
Lomize, J., 1951 [17]	$b^* = b \left[ 1 + 6 \left( \frac{e}{b} \right)^{1.5} \right]^{-1/3}$	b*: Hydraulic opening, b: Mechanical opening, e: Aperture
Louis, P., 1969 [18]	$b^* = b \left[ 1 + 8.8 \left( \frac{e_m}{D_H} \right)^{1.5} \right]^{-1/3}$	b*: Hydraulic opening, b: Mechanical opening, e <sub>m</sub> : Fracture fill, D <sub>H</sub> : Hydraulic diameter
Patir, N., & Cheng, L., 1978 [19]	$b^* = b \left[ 1 + 0.9 \exp \left( -\frac{0.56}{C_y} \right) \right]^{1/3}$	C <sub>y</sub> : Y value, characteristic parameter, b*: Hydraulic opening, b: Mechanical opening
Barton et al., 1985 [20]	$b^* = b^2 JRC^{-25}$	b*: Hydraulic opening, b: Mechanical opening, JRC: Joint Roughness Coefficient,
Olsson, M., & Barton, N., 2001 [21]	$b^* = \frac{b^2}{JRC_0^{0.25}}$ for $u_s \leq 0.75u_{sp}$ $b^* = \sqrt{b} JRC_{mob}$ for $u_s \geq u_{sp}$	b*: Hydraulic opening, b: Mechanical opening, u <sub>s</sub> : Shear displacement, JRC <sub>0</sub> : Joint Roughness Coefficient
Walsh, J., 1981 [22]	$b^{*3} = b^3 \frac{1+C}{1-C}$	b*: Hydraulic opening, b: Mechanical opening, C: Fracture fill parameter
Hakami, E., 1989 [23]	$b^{*2} = \frac{b^2}{C}$	b*: Hydraulic opening, b: Mechanical opening, C: Fracture parameter
Renshaw, C., 1995 [24]	$b^* = b \left( 1 + \frac{\sigma_b^2}{b^2} \right)^{-1/2}$	b*: Hydraulic opening, b: Mechanical opening, σ <sub>b</sub> : Stress
Xie et al. 2015 [25]	$b^{*3} = b^3 \left( 0.94 - 5.0 \frac{\sigma_{bs}^2}{b^2} \right)$	b*: Hydraulic opening, b: Mechanical opening, σ <sub>bs</sub> : Stress parameter

### 3.1.1. Relationship between mechanical and hydraulic openings

Initially, a one-dimensional model was developed using UDEC software. A horizontal joint was introduced into the model at a zero-degree angle, with a spacing of 0.5 meters. The model was then discretized employing the command Gen Edge=0.5.

During the first phase of the Fully Coupled analysis, the fluid was treated as a Compressible Steady State to avoid inputting the bulk modulus, and boundary conditions along with in-situ stress conditions were applied, under the assumption of

no fluid presence within the model. At this stage, mechanical solving was performed, resulting in an imbalance force diagram. Once the forces approached equilibrium, the analysis progressed to the second phase.

In the second phase, hydraulic solving was initiated, transitioning the fluid state from Compressible Steady State to Compressible Transient. Hydraulic boundary conditions were established, and a water head of 1 meter was applied from the left side of the model. This phase activated fluid flow, and the analysis continued using the actual bulk modulus.

Finally, a coupled solution was executed incorporating the actual bulk modulus, allowing for a comparative analysis against the previous stage results, focusing on the defined cycle.

In this study, UDEC software was used to simulate the hydro-mechanical behavior of fractured rock masses and drainage conditions in mining environments. The input parameters for the modeling include the mechanical and hydraulic properties of the rocks and joints, which were carefully selected and calibrated to provide more accurate results in simulating water flow and stress behavior within the mining system. Model calibration and boundary conditions were designed based on geological and hydromechanical data from the Angouran Mine, using standard procedures outlined by Goodman & Shi (1985) [14] to reflect real-world stress distributions and joint behavior.

**Rock Properties:** For modeling the rock mass, an elastic model was employed with a density of 2.7E3 kg/m<sup>3</sup>, and bulk and shear modulus values of 3.62319E9 and 1.9685E9 Pascals, respectively.

**Joint Properties:** Various parameters were used to model the behavior of joints, including a normal

stiffness of 1E9 Pascals and a shear stiffness of 5E8 Pascals. Additionally, a friction coefficient of 25 and permeability of 83 were set for the joints.

**In-Situ Stress Conditions:** To model the real-world conditions of the mine, in-situ stress conditions were incorporated into the model. This includes vertical and horizontal stress values in different directions, simulating the natural and static conditions of the mining environment.

These parameters and assumptions were specifically designed to accurately simulate the water leakage pathways and stress distribution within the fractured rock masses. Consequently, the results obtained from the model are directly comparable to the real-world conditions found in mining environments.

In the initial step, a one-dimensional block is constructed. The subsequent step involves introducing a joint with a zero-degree slope at the center of the model, maintaining a spacing of 1 meter. The third step focuses on discretizing the model, utilizing a zone edge of 0.5. In the fourth step, behavioral models are assigned to both the block and the joint, following the specified codes (Table 4):

**Table 4. The General state of the model before applying hydraulic boundary conditions**

```
group zone 'rock:ID173'
zone model elastic density 2.7E3 bulk 3.62319E9 shear 1.9685E9 range group 'rock:ID173'
group joint 'joint:ID186'
joint model area jks 5E8 jkn 1E9 jfriction 25 jcohesion 1E5 jtension 0 jdilation 0 jperm 83 ares 1E-3 azero 1E-3 range group
'joint:ID186'
;new contact default
set jcondf joint model area jks=5E8 jkn=1E9 jfriction=25 jcohesion=1E5 jtension=0 jdilation=0 jperm=83 ares=1E-3 azero=1E-3
```

In the fifth step, the model transitions from a Compressible Transient state to a Compressible Steady State. The sixth step entails the application of boundary conditions: the bottom of the model is

constrained in both the X and Y directions, while the left and right sides are set to zero in the velocity direction (X). In the seventh step, in-situ stress conditions are introduced to the model (Table 5).

**Table 5. The General state of the model before applying hydraulic boundary conditions**

```
insitu stress -11000.0,0.0,-27000.0 xgrad 0.0,0.0,0.0 ygrad 11000.0,0.0,11000.0 szz -11000.0
zgrad 0.0,11000.0 block pp 0 aperture 0.001 zone pp
```

In the eighth step, gravitational forces are applied to the model. The ninth step involves conducting a mechanical solution with a cycle duration of 3000. In the tenth step, the imbalance forces are calculated.

The eleventh step marks the initiation of the second phase of the analysis, during which the solution is set to the Fluid On state. Initially, boundary conditions for the fluid are defined,

followed by the application of a water pressure corresponding to a 1-meter head on the left side of the model (Table 6). At this stage, both the floor and ceiling of the model are assumed to be impermeable. Subsequently, pore pressure is introduced on the left side of the model.

Figure 1 depicts the model in a fully permeable state, while Figure 2 shows the model with the floor and ceiling rendered impermeable.

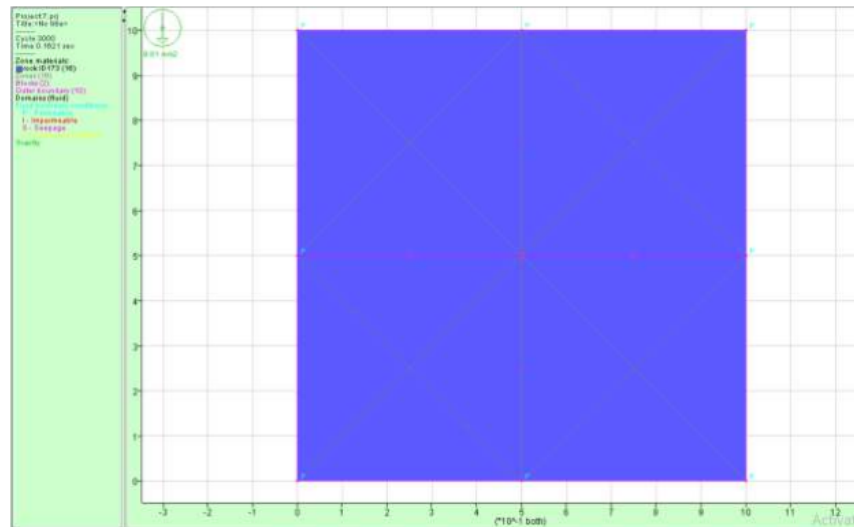


Figure 1. The general state of the model before applying hydraulic boundary conditions

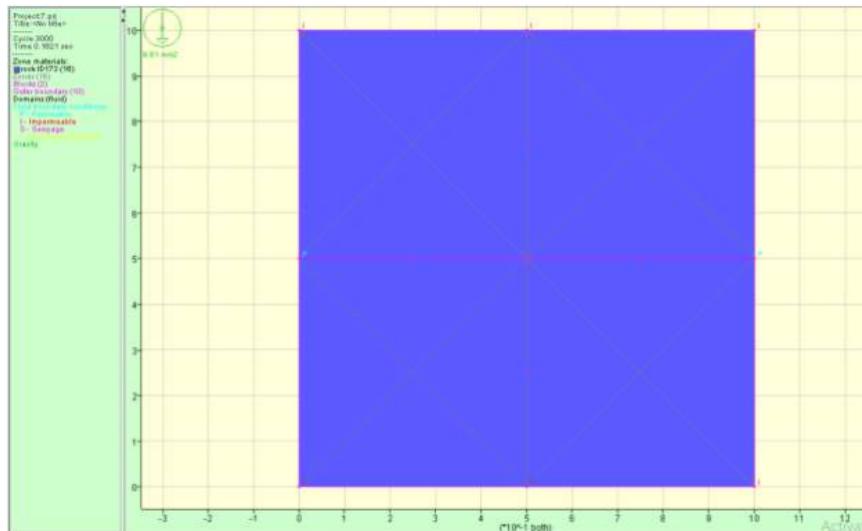


Figure 2. The general shape of the model after applying the hydraulic boundary conditions and the impermeability of the roof and floor of the model

**Table 6. The General state of the model before applying hydraulic boundary conditions**  
 boundary pp 9810.0 pxgrad 0.0 pygrad -9810.0 range -1.366E-2,2.102E-2 -1.036E-2,1.012

In this phase, boundary conditions for pore pressure are applied on the left side of the model according to the specified guidelines. Subsequently, the fluid's bulk modulus and density are defined, and the hydraulic solution for the

model is performed. The outcomes of the hydraulic analysis, conducted within a two-dimensional framework using a one-way coupled approach, are illustrated in Figures 3 and 4.

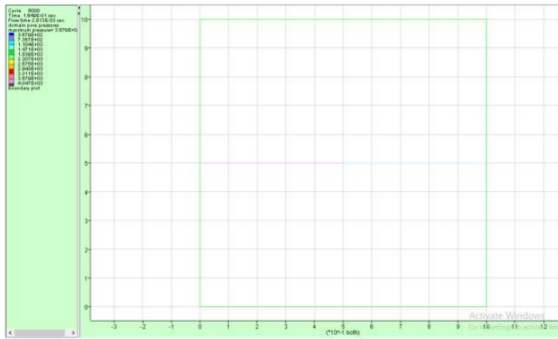


Figure 3. Domain Pore Pressure

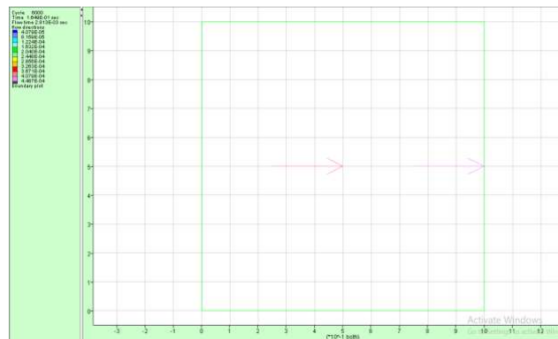


Figure 4. Flow direction vector

Based on the results obtained from the conducted modeling and the analysis of pore water pressure and flow direction vectors, it can be concluded that the modeling was performed with sufficient accuracy. Furthermore, the directions of the outflow vectors correspond well to reality, indicating the validity and reliability of the model in representing the hydro-mechanical processes in the studied environment. This enhances confidence in the analytical results and the practical applicability of the model for predicting water flow behavior under similar conditions. In the next phase, this modeling was applied using actual data and hydro-mechanical conditions from the Angouran Mine, where the obtained results confirmed the model's validity and accuracy in real-world conditions.

### 3.1.2. Numerical Model Implementation in UDEC: Angouran Mine Case Study

In this section, a numerical simulation was conducted to evaluate the hydro-mechanical behavior of the rock mass at the Angouran Lead-Zinc Mine using UDEC software. Angouran Mine is one of the largest lead and zinc producers in Iran and the Middle East (Figure 5), and it is recognized as the first mining tourism site in the country. The objective of the simulation was to simulate the distribution of pore pressure and the mechanical response of the rock mass under applied loading and groundwater flow conditions. The input parameters for the model were derived from field measurements, piezometric data, and geotechnical investigations (Table 7).



Figure 5. Geographical location and view of the Angouran Lead-Zinc Mine in Iran.

**Table 7. Model Input Parameters**

Parameter Type	Value / Description
Rock type	Limestone and dolomite with elastic behavior
Rock density (kg/m <sup>3</sup> )	2700
Young's modulus (Pa)	5×10 <sup>9</sup>
Poisson's ratio	0.27
Joint spacing (m)	5
Joint orientation	0° and 90°
Initial hydraulic aperture (m)	0.001
Joint permeability (mD)	83
Joint normal stiffness (Jkn, Pa)	1×10 <sup>9</sup>
Joint shear stiffness (Jks, Pa)	5×10 <sup>8</sup>
Joint friction angle (°)	25
Applied water pressure (Pa)	4.9×10 <sup>5</sup> (equivalent to 50 m head)
Fluid bulk modulus (Pa)	2×10 <sup>8</sup>
Boundary conditions	Left: pressure; Top/Bottom: impermeable; Right/Bottom: fixed

The model consisted of two orthogonal joint sets (0° and 90°) with regular spacing. Initially, an incompressible transient flow was simulated to evaluate pore pressure and flow direction within the joint network. Subsequently, flow was disabled, and a separate mechanical analysis was performed to assess stress distribution and unbalanced forces under static loading.

The maximum simulated pore pressure was 4.5×10<sup>5</sup> Pa, which closely matched the measured piezometric data from the field (4.4×10<sup>5</sup> Pa), with a relative error of only 2.2%. This indicates a high level of agreement between the model and the real-world conditions (Table 8).

The mechanical analysis results, presented in Figure 6, depict the decline of unbalanced forces and the convergence of the model after 3000 cycles, confirming mechanical equilibrium. As illustrated in Figure 7, the distribution of pore pressure peaks near the left boundary and gradually

decreases toward the right. The flow vectors shown in Figure 8 indicate the dominant flow direction across the joint network, primarily from left to right.

These findings demonstrate that the developed numerical model in UDEC provides an accurate representation of subsurface pressure and flow behavior at the Angouran Mine. It can serve as a reliable tool for designing drainage plans and managing hydrostatic pressure in mining environments.

**Table 8. Comparison of Numerical Modeling Results with Real Data**

Data Type	Maximum Pressure (Pa)
Measured (Piezometric)	4.4×10 <sup>5</sup>
Numerical (UDEC)	4.5×10 <sup>5</sup>
Relative Error	2.2%

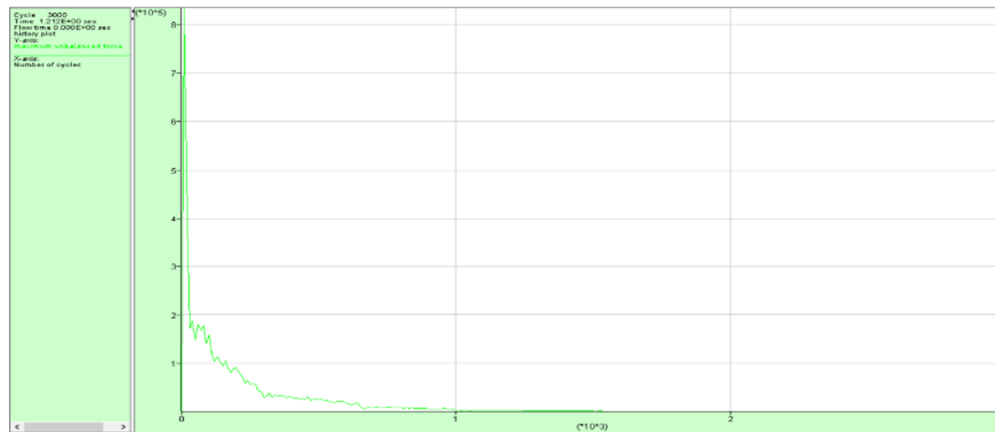


**Figure 6. Unbalanced Forces in the Mechanical Analysis**

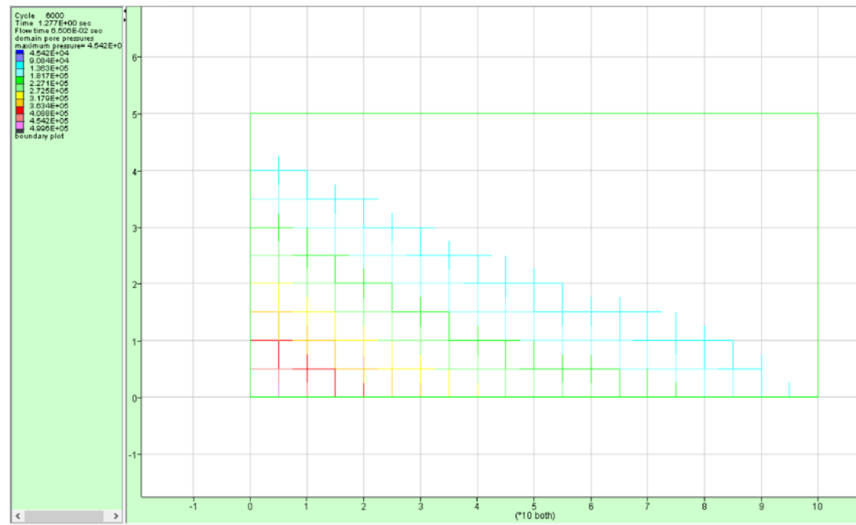


Figure 7. Pore Pressure Range

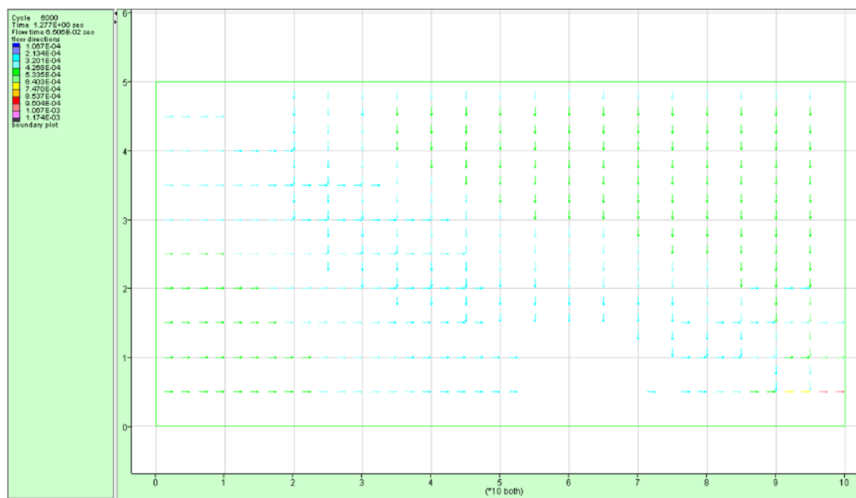


Figure 8. Flow Direction Vectors

### 3.2. Research methodology in the second phase

The study involves a statistical sample of experts in mine drainage, selected from development samples, to provide insights into the parameters crucial for optimizing mine drainage decisions. A network of discontinuities was reconstructed using data collected from these discontinuities. Although the study area is inherently three-dimensional, it was represented through two-dimensional simulations. The Analytic Hierarchy Process (AHP), introduced by Saaty (1980) [26], is one of the most widely used multi-criteria decision-making (MCDM) methods. It provides a structured framework for ranking and prioritizing alternatives based on pairwise comparisons and consistency analysis. Recent advances in mine drainage studies have emphasized the importance of integrating structured decision-making models, particularly

under uncertain and complex mining environments. Ataei (2010a) [27] introduced the fundamental principles of multi-criteria decision-making (MCDM), providing a valuable foundation for structured analysis in mine planning and management. In a complementary volume, Ataei (2010b) [28] expanded this framework by incorporating fuzzy logic into the decision-making process, which is particularly useful for evaluating mine drainage systems under linguistic uncertainty and incomplete or uncertain geotechnical data.

The primary objective of this research is to leverage artificial intelligence to enhance decision-making and manage risks associated with leakage in rock mass environments. By utilizing available mine data, including permeability and water head, the hydraulic conditions were simulated, leading to outputs related to leakage and water head. The AHP methodology in this study follows the foundational

framework proposed by Saaty (1980) [26], where pairwise comparisons, consistency ratios, and weight derivation are calculated systematically to ensure objectivity and rationality in decision-making.

The environments analyzed include continuous, porous, and dual-porous settings, with a focus on modelling leakage within these porous structures. Previous studies on fluid flow in rock masses have examined the effects of various factors such as hydraulic gradient, intersection angle, surface roughness, and aperture size, as well as the influence of scale on unit fractures. This study aims to analyze and simulate the environments in question while gathering input from mine drainage experts. Based on the leakage model and the resulting outputs, and considering aspects like cost reduction, physical drainage challenges, and economic conditions, a drying strategy is proposed. Additionally, this phase of the project emphasizes the application of soft computing techniques, including genetic algorithms, neural fuzzy systems, and artificial intelligence. The dynamic decision-making model presented in this research will be continuously updated to operate intelligently (Figure 9).

**3.2.1. Research methodology in the second phase**

A questionnaire was developed and distributed to research experts to assess the significance of various indices using linguistic variables. The

findings from this survey are presented in **Table 9**. Upon collecting the completed questionnaires, the responses were compiled into a table reflecting the experts' evaluations. These evaluations were then translated into numerical values using a predefined conversion table, enabling the calculation of weights for each index. The calculated results are summarized in **Table 10**. In this phase, expert-based decision analysis was conducted using the principles of the Analytic Hierarchy Process (AHP), whereby qualitative linguistic judgments were converted into numerical weights to determine the relative importance of quality indicators.

**3.2.2. Evaluating the importance of options according to qualitative indicators and normalizing the decision matrix**

Experts were invited to complete a questionnaire utilizing linguistic (verbal) variables, rating their evaluations on a scale from zero to ten, as outlined in the table below (**Table 11**). Subsequently, a decision-making matrix was developed based on the research methodology, incorporating the experts' opinions. The elements of this decision matrix are detailed in the following **table 11**. The normalized matrix was generated by applying normalization procedures to both the matrix of direct relationships and the decision matrix. In this analysis, the positive indicators identified are quality (Q2) and safety (Q4), whereas the negative indicators are time (Q1) and cost (Q3).

**Table 9. Determining the weight of quality indicators**

Expert index	Q1	Q2	Q3	Q4	Expert index	Q1	Q2	Q3	Q4
D1	VH	L	VH	MH	D17	L	VL	VH	L
D2	VH	ML	VH	MH	D18	ML	H	VH	ML
D3	VH	ML	H	L	D19	VH	MH	VH	H
D4	H	MH	VH	ML	D20	ML	VH	H	M
D5	VH	MH	VH	MH	D21	MH	H	MH	MH
D6	H	MH	H	MH	D22	H	VH	H	L
D7	VH	MH	VH	MH	D23	MH	L	H	ML
D8	VH	MH	VH	H	D24	ML	ML	MH	MH
D9	VH	H	VH	M	D25	MH	MH	VH	MH
D10	VH	M	VH	H	D26	M	M	H	MH
D11	H	MH	H	MH	D27	MH	ML	MH	H
D12	ML	ML	VH	MH	D28	H	MH	MH	M
D13	MH	MH	VH	H	D29	H	M	H	H
D14	H	M	VH	H	D30	MH	M	H	MH
D15	H	H	VH	MH	D31	H	L	MH	MH
D16	MH	L	H	MH	D32	MH	MH	VH	H

Symbol Explanation: **Q1, Q2, Q3, Q4**: These represent the different levels of quality indicators. The classification is as follows: Q1: Low quality, Q2: Medium-low quality, Q3: Medium quality, Q4: High quality. VH (Very High): Very High, H (High): High, M (Medium): Medium, ML (Medium-Low): Medium-Low, L (Low): Low, VL (Very Low): Very Low, Expert index: This index reflects the evaluation of experts in the context of quality indicators or other relevant characteristics. It is often used to represent an overall quality or score based on expert assessment. D1, D2, ..., D32: These are identifiers for specific data points or indicators used in the table. Each corresponds to a specific parameter or factor under consideration in the analysis.

**Table 10. The linguistic equivalent weight of indicators according to experts**

Expert index	Q1				Q2				Q3				Q4				Expert index	Q1				Q2				Q3				Q4			
D1	0/9	1	0/1	0/3	0/9	1	0/6	0/7	D17	0/1	0/3	0	0/1	0/9	1	0/1	<b>0/3</b>																
D2	0/9	1	0/3	0/4	0/9	1	0/6	0/7	D18	0/3	0/4	0/7	0/9	0/9	1	0/3	<b>0/4</b>																
D3	0/9	1	0/3	0/4	0/7	0/9	0/1	0/3	D19	0/9	1	0/6	0/7	0/9	1	0/7	<b>0/9</b>																
D4	0/7	0/9	0/6	0/7	0/9	1	0/3	0/4	D20	0/3	0/4	0/9	1	0/7	0/9	0/4	<b>0/6</b>																
D5	0/9	1	0/6	0/7	0/9	1	0/6	0/7	D21	0/6	0/7	0/7	0/9	0/6	0/7	0/6	<b>0/7</b>																
D6	0/7	0/9	0/6	0/7	0/7	0/9	0/6	0/7	D22	0/7	0/9	0/9	1	0/7	0/9	0/1	<b>0/3</b>																
D7	0/9	1	0/6	0/7	0/9	1	0/6	0/7	D23	0/6	0/7	0/1	0/3	0/7	0/9	0/3	<b>0/4</b>																
D8	0/9	1	0/6	0/7	0/9	1	0/7	0/9	D24	0/3	0/4	0/3	0/4	0/6	0/7	0/6	<b>0/7</b>																
D9	0/9	1	0/7	0/9	0/9	1	0/4	0/6	D25	0/6	0/7	0/6	0/7	0/9	1	0/6	<b>0/7</b>																
D10	0/9	1	0/4	0/6	0/9	1	0/7	0/9	D26	0/4	0/6	0/4	0/6	0/7	0/9	0/6	<b>0/7</b>																
D11	0/7	0/9	0/6	0/7	0/7	0/9	0/6	0/7	D27	0/6	0/7	0/3	0/4	0/6	0/7	0/7	<b>0/9</b>																
D12	0/3	0/4	0/3	0/4	0/9	1	0/6	0/7	D28	0/7	0/9	0/6	0/7	0/6	0/7	0/4	<b>0/6</b>																
D13	0/6	0/7	0/6	0/7	0/9	1	0/7	0/9	D29	0/7	0/9	0/4	0/6	0/7	0/9	0/7	<b>0/9</b>																
D14	0/7	0/9	0/4	0/6	0/9	1	0/7	0/9	D30	0/6	0/7	0/4	0/6	0/7	0/9	0/6	<b>0/7</b>																
D15	0/7	0/9	0/7	0/9	0/9	1	0/6	0/7	D31	0/7	0/9	0/1	0/3	0/6	0/7	0/6	<b>0/7</b>																
D16	0/6	0/7	0/1	0/3	0/7	0/9	0/6	0/7	D32	0/6	0/7	0/6	0/7	0/9	1	0/7	<b>0/9</b>																
W1	0.65				0.79				W3	0.79				<b>0.92</b>																			
W2	0.47				0.61				W4	0.53				<b>0.68</b>																			

Symbol Explanation: Q1, Q2, Q3, Q4: These columns represent the quality levels as assessed by experts. The values in these columns are the corresponding weights assigned to these quality levels. The classification is as follows: Q1: Low Quality, Q2: Medium Quality, Q3: High Quality, Q4: Very High Quality. Expert Index: This index is an aggregated score based on expert evaluations of the indicators. The expert index reflects the overall quality weight attributed to each indicator based on expert judgment. Weight Values (e.g., 0/3, 0/1, 1, 0/7, etc.): These numbers represent the linguistic equivalent of the quality levels assigned to each indicator. These values correspond to the weight or degree of importance that each indicator holds in the evaluation process (For example, a value of 0/9 represents a low quality, whereas 1 indicates the highest possible value for a given indicator's weight.). D1, D2, D3, ..., D32: These are identifiers for different data points or indicators used in the table. They refer to specific quality indicators being assessed based on expert evaluations. W1, W2, W3, W4: These represent weights that have been calculated for specific criteria or sets of data, typically derived from the overall evaluation of each indicator's quality level.

**Table 11. Normalization of the decision matrix**

7	8.8	3.7	4.8	6.2	7.3	6.9	8.8	7	9	6.1	7.13	4	5.6	3.8	4.8	8.9	10	3.6	4.7	6.5	7.5
5.6	6.6	3.8	4.8	5.7	6.8	3.9	5.9	6.4	8.3	1.8	3.6	8.2	9.3	6.7	8.5	5.8	6.8	8.3	9.3	6.5	8.2
7.3	9	8.6	9.7	8.7	9.8	8.8	9.9	8.6	9.7	7.3	9.1	8.5	9.7	8.7	9.8	8.8	9.9	6.9	8.9	6.6	7.7
5.9	7.1	5.7	6.8	6.9	8.8	6.9	8.8	5.9	7	6	7.3	2.2	4.1	3.2	4.3	6.4	8.3	4.1	5.9	5.4	6.6
11	12	13	14	15	16	17	18	19	20	21											
G1	8.1	9.2	8.8	9.9	8.9	9.9	7.3	9.1	8.8	9.9	7.3	9	8.8	9.9	8.7	9.8	8.8	9.9	8.4	9.6	
G2	3.5	5.1	3.4	4.5	3.9	4.9	5.8	6.9	5.4	6.4	5	6	5.7	6.7	5.7	6.7	5.9	7.4	4.3	5.8	
G3	7.9	9.1	8.4	9.6	7.3	9.1	8.6	9.8	8.2	9.5	7.4	9.1	8.7	9.8	8.5	9.7	8.5	9.7	8.6	9.8	
G4	5.8	7	5.7	6.8	1.5	3.4	3.1	4.2	5.8	6.8	5.5	6.7	5.8	6.8	6.5	8.4	3.7	5.7	6.7	8.5	
1	2	3	4	5	6	7	8	9	1												
7	8.9	6.2	7.3	3.5	4.6	6.3	7.3	4.5	6.4	5.9	7.1	6.9	8.9	7	9	6	7	6.8	8.8	6	7
8.4	9.4	4.2	4	3.4	4.4	5.9	6.9	4.4	6.1	9.3	4.5	5.8	6.8	4	6	4.2	6.2	1.6	3.5	5.9	6.9
7	8.9	7.3	9.1	6.5	7.7	8.8	9.8	7.1	8.9	6.2	7.3	6.4	7.4	7	9	7	9	6.1	7.3	8.8	9.8
1.7	3.5	3.3	4.4	5.7	6.7	5.7	6.7	5.8	6.8	6.6	8.5	3.9	5.9	6.7	8.7	6	7	5.8	6.8	6.5	8.5
22	23	24	25	26	27	28	29	30	3	1	32	33									
3.9	5.1	8.5	9.7	3.4	4.5	4.3	6.2	6.4	8.2	6	7.1	3.4	4.6	6.1	7.3	6.3	7.4	7.3	9.1	6.3	7.3
3.8	4.8	8.4	9.4	6.5	8.4	4.1	5.9	6.1	7.3	7.8	8.9	6.3	8.2	7.7	8.7	2.4	4.2	3.8	4.8	5.9	6.9
6.2	7.3	6.3	7.4	6.7	8.5	5.1	6.9	6.3	7.3	6.6	7.6	7	9	6.9	8.7	6.3	7.5	9	10	7.3	9.1
5.8	6.8	5.7	6.8	2.1	4.1	3.6	4.6	6.8	8.6	6.2	7.3	6.1	7.3	1.9	3.8	3.5	4.6	6.7	8.3	5.8	6.9
34	35	36	37	38	39	40	41	42	43	44											
4	5.1	6.4	7.5	3.8	5	6	7.1	4.5	6.4	6.1	7.3	7.1	9.1	7.1	9.1	6.1	7.1				
4.4	6.2	3.6	4.7	6	7.1	2	3.8	3.5	4.5	3.3	4.4	6.1	7.1	6.1	7.1	6.0	7				
6.4	7.4	8.8	9.9	8.7	9.8	8.7	9.8	7	8.8	6.4	7.4	7.1	9	8.9	9.9	8.8	9.8				
6.1	8.1	6.0	6.9	5.6	6.7	6.7	8.3	6.4	8.3	6	7.1	6.1	7	1.7	3.5	3.9	5.8				
45	46	47	48	49	50	51	5	2	53												
7	8.9	6.2	7.3	3.5	4.6	6.3	7.3	4.5	6.4	5.9	7.1	6.9	8.9	7	9	6	7	6.8	8.8	6	7
8.4	9.4	4.2	4.0	3.4	4.4	5.9	6.9	4.4	6	9.3	4.5	5.8	6.8	4.0	6.0	4.2	6.2	1.6	3.5	5.9	7
7.0	8.9	7.2	9.1	6.5	7.7	8.8	9.8	7.1	8.9	6.2	7.3	6.4	7.4	7	9	7	9	6.4	7.1	8.8	9.8

**3.2.3. Determining the best positive option (the best possible answer) for comparing the decision-making method**

Among the available options, it is essential to identify the most significant risk for each indicator as the primary focus. This approach enables the evaluation of the likelihood of each risk affecting the time, cost, quality, and safety indicators. Ultimately, it is also necessary to assess the overall impact of these identified risks on the project (Table 12).

**Table 12. Determining the best positive option**

VQ MAX		
V1	0.54	0.79
V2	0.42	0.61
V3	0.58	0.92
V4	0.41	0.6

**Symbols Explanation:** VQ MAX: Represents the maximum value of the Value of Quality (VQ) for each option. It indicates the highest achievable score related to the quality or effectiveness of each alternative in addressing specific project indicators such as time, cost, quality, and safety. V1, V2, V3, V4: These are the options or alternatives being evaluated. Each option represents a distinct strategy, solution, or approach under consideration. Values (e.g., 0.54, 0.79, etc.): The numerical values in the table indicate the respective scores for each option. These scores are derived from assessments of how well each option performs with respect to the evaluated indicators. For example: V1 =

0.54, 0.79: Option V1 has a quality score of 0.54, with a maximum achievable value of 0.79. V3 = 0.58, 0.92: Option V3 has the highest maximum quality value of 0.92, indicating that it performs best among the options.

**3.2.4. Quantifying the intensity of the effect on the four indicators**

Based on the responses from participants, the degree of closeness of each option to the optimal choice in their rankings was assessed. In the context of risk evaluation, two critical factors—impact intensity and likelihood of occurrence—illustrate the effects of associated risks. Therefore, both elements should be incorporated into the calculations. To facilitate this, the impact of each project goal was quantified across five levels, using a scale from 1 (lowest) to 5 (highest), as defined by the American Project Management Standard 2012. A crucial aspect of this process is the numerical value assigned in the rating section for each identified risk (Table 13).

**3.2.5. Probability of risk in decision making for drainage in mines**

The opinions of the respondents regarding the potential occurrence of risks in the decision-making process for optimal drainage are presented, along with the average probabilities of the outcomes obtained, as illustrated in the table 14.

**Table 13. Quantification of the intensity of the effect on the project goals**

intended purpose	Very low 0.1-0.3	Low 0.3-0.5	Average 0.5-0.7	Much 0.7-0.9	Too much 0.9-1
1 time (relative to the initial time)	increase	Less than 5% increase	5-10% increase	10-20% increase	More than 20%
2 Quality (compared to the standard and technical specifications)	insignificant	It only affects some functions of the project	It is acceptable to accept the reduction of quality by obtaining the permission of the shareholder	Quality reduction	Increase The goals of the project are flawed
3 Cost (relative to the estimated cost)	Somewhat reduced	Less than 10% increase	10-20% increase	For the shareholder	More than 40%
4 safety	increase	Somewhat dangerous	dangerous	It is not acceptable	afoul
Assigned numerical value	80%	40%	20%	10%	5%

**Table 14. Risk probability**

row	Risk item	Possibility	row	Risk item	Possibility
1	Exchange rate change	54.1%	28	Insufficient financial capacity of the contractor	48.4%
2	Improper human resource incentive/maintenance or punishment systems	59.1%	29	Weak managerial ability and coordination of the contractor	50.9%
3	Lack of familiarity and use of modern execution methods	57.8%	30	Moving and leaving jobs by key personnel	49.1%
4	Lack of senior management support for planning requirements	49.1%	31	Improper organization of personnel	51.6%
5	Lack of access to drainage records in similar mines	52.2%	32	Failure to use management processes	54.7%
6	Lack of necessary coordination and support of the headquarters departments for drainage in mines	54.1%	33	Lack of access to materials and materials	61.6%
7	Lack of systemic attitude among the departments related to drainage in mines	56.6%	34	Ignorance in observing safety principles and improper training of workers	64.1%
8	Incomplete or incorrect feasibility and economic studies	50.3%	35	Inadequate monitoring of the quality of executive activities	51.6%
9	Inefficiency of management information systems in drainage in mines	54.7%	36	Damage during transportation	54.7%
10	Delay in obtaining permits and creating coordination (administrative bureaucracy)	46.6%	37	Delay in transporting equipment	50.9%
11	sanctions / war	54.1%	38	Delay in the construction of equipment	54.1%
12	Changes in laws and regulations	55.3%	39	Improper quality control in equipment manufacturing	50.3%
13	Low quality materials and materials	52.2%	40	Design problems and changes in implementation plans in the implementation phase	54.1%
14	Theft and theft of installed equipment	55.3%	41	Using design methods and standards	52.2%
15	Inappropriate industrial culture of the workforce	55.3%	42	Inappropriate	52.2%
16	Pipeline intersection with old buried pipes	55.6%	43	Delay or shortfall in delivery of executive plans	60.3%
17	The intersection of the pipeline route with existing roads, railways and highways and crossing them	54.7%	44	Failure to use value engineering in the design phase	59.7%
18	Climatic and weather conditions, type of flooding, snow, blizzard or torrential rains	47.2%	45	Management attitude in reducing the time of the design phase and fast transition to the implementation phase	50.3%
19	Fire and unexpected events including terrorist explosions in the direction of drainage in mines	50.3%	46	Delay in concluding a contract and solving contractual issues	56.6%
20	Damage to materials and drainage equipment in mines	50.3%	47	Imposing a tight schedule on the contractor	51.6%
21	Mistake in timing and sequence of drainage activities in mines	55.3%	48	Executive changes during work to order	47.2%
22	Wrong estimate/meter to provide the price in the tender	55.3%	49	the employer	52.8%
23	Poor labor productivity	52.2%	50	Interferences and law violations by the employer	55.9%
24	Weak workshop equipment (machines and equipment)	53.4%	51	Solving issues related to land acquisition in the direction of drainage in mines	55.3%
25	Improper allocation of manpower and equipment	55.9%	52	Managers' abuses of drainage resources in mines	52.8%
26	Exceeding the approved implementation methods	53.4%	53	Lack of liquidity and delay in payment of statements of status with the contractor	58.4%
27	Exceeding the scope and terms of the contract	54%	54		

### 3.2.6. Multicriteria Decision-Making Model Based on AHP

In this study, the Analytic Hierarchy Process (AHP) was employed as the multicriteria decision-making (MCDM) method to determine the weight of indicators influencing decision-making in mine drainage management. Introduced by Saaty (1980) [26], AHP is recognized as one of the most structured and widely used techniques for solving complex decision problems.

In the initial phase, the quality indicators were evaluated by experts across four levels: Q1 (Low), Q2 (Medium), Q3 (High), and Q4 (Very High). These evaluations were conducted using linguistic variables such as "Low," "High," and "Very High." The qualitative responses were then converted into numerical values ranging from 0 to 1 using a predefined linguistic-to-numeric scale.

A pairwise comparison matrix was constructed, and the final weights for each quality level were calculated using the geometric mean method. The

average weights for the four quality levels are presented in **Table 15**:

**Table 15. Average Weights of Quality Levels and Final Expert Index Based on Expert Evaluations**

Quality Level	Average Weight
Q1 (Low)	0.576
Q2 (Medium)	0.588
Q3 (High)	0.514
Q4 (Very High)	0.603
Expert Final Index	0.596

The final expert index, calculated by aggregating the weights of the four quality levels, was 0.596. This reflects a relatively conservative and convergent approach in expert judgments, contributing to the reliability and precision of the final decision-making process.

**3.2.7. Pairwise Comparison Matrix and Final Weight Calculation of Quality Indicators**

To determine the relative importance of each quality level (Q1 to Q4), a pairwise comparison matrix was constructed based on expert evaluations. These comparisons were initially

**Table 17. Final Weights of Quality Levels Calculated Using the Geometric Mean Method (AHP)**

Criterion	Geometric Mean	Normalized Final Weight
Q1	0.759	0.153
Q2	1.414	0.285
Q3	0.759	0.153
Q4	2.289	0.409

These weights indicate that Q4 (Very High Quality) with a weight of 0.409 and Q2 (Medium Quality) with 0.285 are the most influential criteria in the overall quality assessment.

**3.2.9. Consistency Evaluation**

To ensure the internal consistency of the pairwise comparisons, the Consistency Index (CI) and the Consistency Ratio (CR) were calculated:

- **Consistency Index (CI):** 0.022
- **Random Index (RI) for n = 4:** 0.90
- **Consistency Ratio (CR) = CI / RI:** 0.024

Since the CR value is less than 0.1, the matrix is considered **acceptably consistent** and the judgments are deemed reliable.

**3.3. Machine Learning Models in the third phase**

In many engineering and environmental projects, accurate prediction of water flow rates is

made using linguistic terms and were subsequently converted to numerical values according to Saaty's Fundamental Nine-Point Scale. The pairwise comparison matrix for the quality criteria is presented in **Table 16**:

**Table 16. Pairwise Comparison Matrix of Quality Levels Based on Expert Judgments (AHP Method)**

	Q1	Q2	Q3	Q4
Q1	1	1/2	1	1/3
Q2	2	1	2	1/2
Q3	1	1/2	1	1/3
Q4	3	2	3	1

**Note:** This matrix was derived from the relative values indicated by expert assessments in Tables 7 and 8. It reflects that Q2 (Medium Quality) and Q4 (Very High Quality) were generally considered more important than Q1 and Q3.

**3.2.8. Weight Calculation Using the Geometric Mean Method**

The geometric mean of each row was calculated, followed by normalization to derive the final weights for each quality level (**Table 17**):

essential for water resource management and future condition forecasting. Piezometric data, which precisely measure groundwater levels at various points, can serve as valuable inputs for predictive models. Studies have demonstrated the critical role of piezometric data in improving the accuracy of hydrological modeling and supporting water resource management strategies [29].

Machine learning models, especially those designed for simulating and predicting complex and nonlinear behaviors, have found significant applications in this field. The primary objective of this study is to predict flow rates in a hydrological system using piezometric data [30]. For this purpose, three machine learning methods—including linear, nonlinear, and artificial neural network (ANN) models—have been employed, and a comparative analysis has been conducted to evaluate their performance in predicting flow rates.

In this study, the implementation of the linear, nonlinear, and ANN models is complemented by a performance evaluation using various statistical metrics. These metrics include the coefficient of

determination ( $R^2$ ), mean absolute error (MAE), root mean square error (RMSE), and mean absolute percentage error (MAPE), each of which provides insights into the accuracy and reliability of the model's predictions. At this stage, the flow rate is predicted precisely and effectively based on piezometric data, enabling experts and engineers to make more informed decisions in water resource management and develop detailed dewatering plans.

The importance of this study becomes more evident when considering its practical applications. Predicting flow rates using machine learning models can be highly beneficial in hydrology projects, civil engineering, water resource management, and urban planning. For instance, these predictions can help prevent crises caused by sudden changes in groundwater levels [31] or optimize the design of water-related projects, such as canal construction. Furthermore, piezometric data, which provide accurate measurements of water levels, deliver highly precise information that facilitates swift and effective decision-making [32].

### 3.3.1. Linear Machine Learning Model

The linear model is one of the simplest yet most widely used models in machine learning, specifically designed for predicting numerical values. This model assumes that the relationship between input variables (features) and the output variable (prediction) is linear. In other words, the model's output is a linear combination of the inputs. For instance, if  $x_1, x_2, \dots, x_n$  are the input features, the model's output can be expressed in **Equation 1** as follows ([33]; [34]):

$$y = w_0 + w_1x_1 + w_2x_2 + \dots + w_nx_n \quad (1)$$

Where:

$y$ : predicted output variable,

$w_0$ : intercept or bias, adjusting the output when all input features are zero,

$w_1, w_2, \dots, w_n$ : coefficients, each representing the impact of the corresponding input feature on the output prediction,

$x_1, x_2, \dots, x_n$ : input features influencing the output prediction.

A linear model assumes that changes in the features are related to the output through a linear relationship, which contributes to the simplicity and computational efficiency of the modeling process.

### 3.3.2. Polynomial Regression

Polynomial Regression builds upon linear regression by incorporating polynomial terms of the independent variables. This extension allows the model to capture non-linear relationships between the variables, providing a better fit for datasets where such relationships exist. The advantage of polynomial regression is that it offers more flexibility compared to linear models, making it suitable for environmental predictions where patterns often deviate from linearity. However, the inclusion of higher-degree terms can lead to overfitting, especially in small datasets, making the model highly sensitive to noise and less generalizable to new data [35]. Thus, while polynomial regression improves accuracy, careful tuning is necessary to prevent overfitting.

Polynomial regression is a type of regression technique used for modeling nonlinear relationships between input features and the target variable. Unlike linear models, which assume a linear association between inputs and outputs, polynomial models are capable of capturing more complex and nonlinear interactions. This is achieved by incorporating higher-order terms (such as squared or cubic features) into the model, allowing it to simulate nonlinear patterns in the data. A polynomial regression model assumes that the relationship between the features and the output can be expressed as a combination of different powers of the input variables. For instance, for a set of features  $x_1, x_2, \dots, x_n$ , a second-degree polynomial model may be formulated as follows:

---


$$y = w_0 + w_1x_n + w_2x_2 + \dots + w_nx_n + w_1^2x_{n+1} + w_2^2x_{n+2} + \dots \quad (2)$$


---

Where:

$y$  is the predicted output (dependent variable),

$x_1, x_2, \dots, x_n$  are the input features (independent variables),

$w_0$  is the intercept term,  $w_1, w_2, \dots, w_n$  are the coefficients corresponding to the original input features,

$w_1^2, w_2^2, \dots$  represent the squared weights (not features), used as coefficients for extended transformed features  $x_{n+1}, x_{n+2}, \dots$  which are often

nonlinear transformations of the original inputs (e.g., squared or interaction terms).

As shown in Equation (2), in addition to the original input features, the model includes their second-degree (squared) terms. This structure allows the model to better capture complex, nonlinear relationships in the data.

Polynomial regression, therefore, serves as a flexible extension of linear models, particularly effective when the relationship between input and output variables involves curvature or other nonlinear dynamics [35].

### 3.3.3. Artificial Neural Networks (ANNs)

Artificial Neural Networks (ANNs) are a class of machine learning models inspired by the structure of the human brain. They consist of layers of interconnected nodes, or “neurons,” where each neuron processes input through a mathematical function and passes the output to the next layer. A typical ANN includes an input layer, one or more hidden layers, and an output layer. This architecture enables ANNs to approximate complex and highly nonlinear relationships in the data.

In environmental and hydrological modeling, ANNs are particularly effective because they can learn patterns from large, multidimensional datasets without requiring predefined assumptions about the form of the relationships. For instance, they can model how changes in groundwater levels—affected by time, geology, and weather—impact flow rates, even when such relationships are nonlinear and dynamic.

However, ANNs require careful training and hyperparameter tuning to avoid overfitting, especially when datasets are small or noisy. They also typically demand greater computational resources compared to simpler models like linear regression ([36]; [37]).

### 3.3.4. Piezometric Data from Angouran Mine

In this study, piezometric data from the Angouran Mine, located in Zanjan County, Iran, were utilized. The piezometric data, which were collected from various piezometers installed across the mine site, provide detailed measurements of groundwater levels and are instrumental in predicting flow rates and supporting resource management strategies. The coordinates of the piezometers at the Angouran Mine are presented in **Table 18**. The water level relative to local coordinates is illustrated in **Figure 10**, while the water level relative to the borehole collars at the Angouran Mine is depicted in **Figure 11** [38].

**Table 18. The coordinates of the piezometers at the Angouran Mine [38]**

	Z	Y	X
<b>P01</b>	2988	1189	1649
<b>P02</b>	3023	1691.47	876.043
<b>P03</b>	3056.45	1726.94	323.843
<b>P04</b>	3081.34	1432.4	92.294
<b>P05</b>	2980.45	993.974	-248.119
<b>P06</b>	2963	145	-178
<b>P07</b>	2959	-158	-2
<b>P08</b>	2789	-511	1027

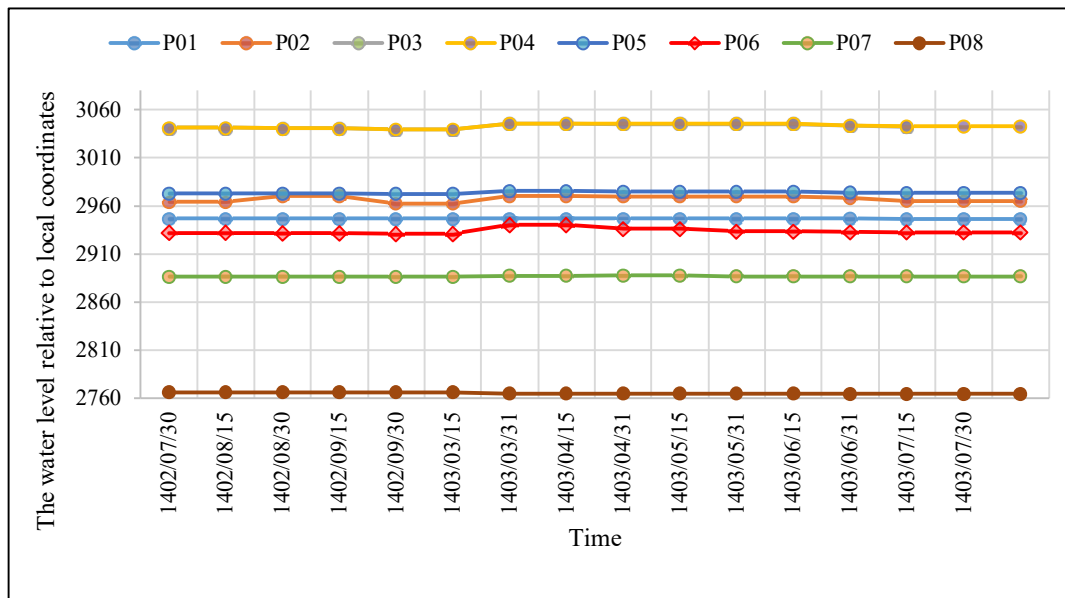


**Figure 10. The water level relative to local coordinates [38]**

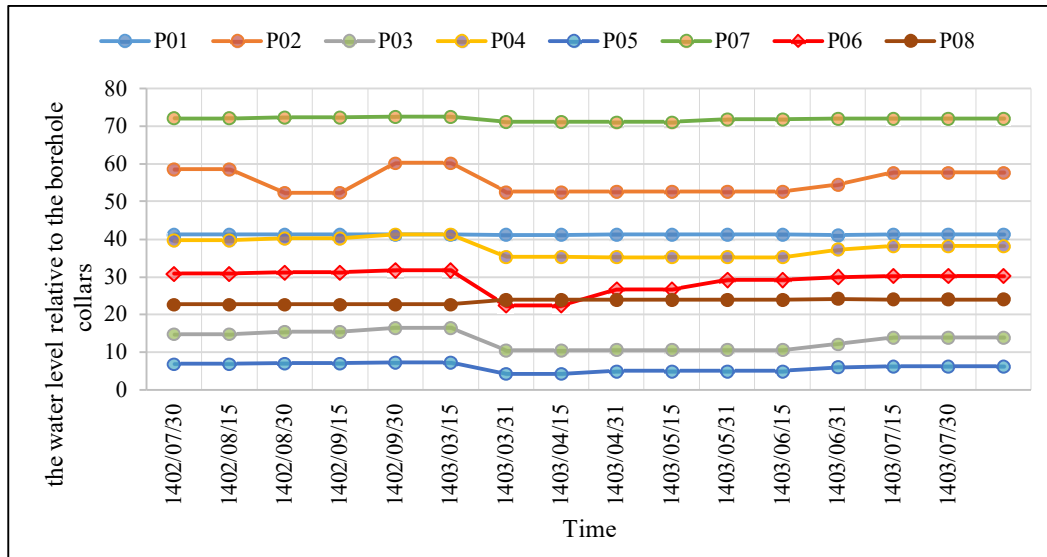


Figure 11. The water level relative to the borehole collars [38]

Figure 10 illustrates the fluctuations in water levels relative to local coordinates over a specified time period. Monitoring points (P01 to P08) exhibit varying water levels, with points P04 and P05 recording the highest levels and showing minimal fluctuations. Point P07 maintains the lowest water level throughout the period, with an almost constant trend. At point P06, slight downward changes are observed. Overall, the pattern of fluctuations indicates relative stability in water levels at most points, with minor short-term variations.

Figure 11 depicts the changes in water levels relative to the borehole collars, revealing distinct upward and downward trends. Points P02 and P07 exhibit the highest water levels, with P07 remaining nearly constant, while P02 shows a declining trend. Conversely, points P01 and P03 record the lowest levels, with a noticeable downward trend. At point P06, a sudden drop is observed, followed by a gradual upward trend. These variations reflect the influence of environmental and hydrological factors on the distribution of water levels in the boreholes.

Prior to model training, the dataset was cleaned and normalized. The data was split into 70% training and 30% testing subsets, and cross-validation was performed to ensure model generalization.

### 3.3.5. Implementation of a Linear Model in MATLAB for Flow Rate Prediction Based on Piezometric Data

In MATLAB, a linear model can be implemented using the `fitlm` function, which is

designed for linear regression. This function uses input data to train the model and then determines the model coefficients using the Ordinary Least Squares (OLS) method [39].

The steps for implementing the linear model are outlined as follows:

- 1. Input Data:** The input data includes the features and outputs used for training the model. It is assumed that the data is provided in the form of a table or matrix [39].
- 2. Model Training:** Using the training data, the linear model is constructed. This step involves selecting the features as model inputs and the output for prediction [40].
- 3. Output Prediction:** After training the model, it can be used to predict new values. For this purpose, the `predict` function is employed, which provides predictions based on new input features [39].
- 4. Model Evaluation:** To assess the performance of the linear model, various metrics can be used, such as the coefficient of determination  $R^2$ , the mean absolute error (MAE), and the root mean square error (RMSE) [34].

In the case of linear regression, significant deviations from actual values were observed, especially in regions with higher flow rates. These discrepancies highlight the model's underperformance in capturing the more complex, non-linear relationships that are inherent in groundwater flow dynamics. Linear regression, being a relatively simple model, struggled to adapt to the variability present in the data, resulting in predictions that did not fully capture the fluctuations in flow rates, particularly in high-flow scenarios. This indicates that linear regression is

less effective for predicting flow rates in environments where non-linearities dominate. As shown in Figure 12, there is a clear deviation between predicted and actual values, particularly in high-flow areas, confirming the model's limitations.

### 3.3.6. Implementation of a Polynomial (Nonlinear) Model in MATLAB for Flow Rate Prediction Based on Piezometric Data

A polynomial (nonlinear) model can be implemented in MATLAB by expanding the feature matrix with second-degree terms. This involves calculating the square of each input feature and appending them to the original feature set for both training and test data, resulting in  $X_{poly\_train}$  and  $X_{poly\_test}$ .

The model is then trained using the *fitlm* function, with  $X_{poly\_train}$  as the input and the corresponding target values as output. Once trained, the model is used to predict outcomes for the test set using  $X_{poly\_test}$ .

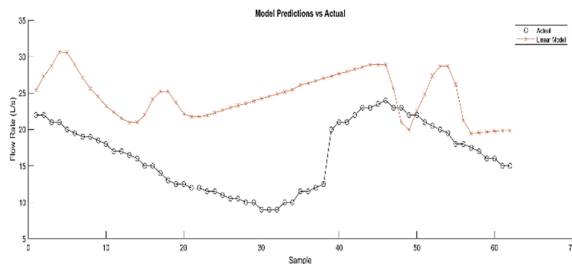


Figure 12. Comparison chart of linear model prediction and actual data

### 3.3.7. Implementation of an Artificial Neural Network (ANN) in MATLAB for Flow Rate Prediction Based on Piezometric Data

In MATLAB, an Artificial Neural Network (ANN) can be implemented using the *fitnet* function, which is designed for function fitting and regression tasks. A common configuration involves defining a network with two hidden layers, each containing 10 neurons. The network is trained using the *train* function with the input and output training data.

The key implementation steps are summarized as follows:

1. **Network Definition:** A feedforward neural network with two hidden layers (each with 10 neurons) is created using *fitnet([10 10])*.

Model performance is evaluated by comparing the predicted values with actual outputs using common error metrics such as  $R^2$ , MAE, and RMSE. This method allows the model to capture nonlinear patterns in the data more effectively than a simple linear approach.

The polynomial regression model showed better alignment with actual values compared to linear regression, particularly in the mid-range flow rates. By incorporating higher-degree polynomial terms, this model was able to capture some of the non-linear relationships between the input variables and the predicted flow rates. As a result, the predictions were more accurate and reflected the data's complexity more effectively than the linear model. However, while the polynomial regression improved upon the linear model, its performance still varied at the extreme ends of the flow rate spectrum, where more sophisticated models were needed. This improvement in prediction accuracy is illustrated in Figure 13, where polynomial regression predictions are closer to the actual data, particularly in the mid-range flow rates.

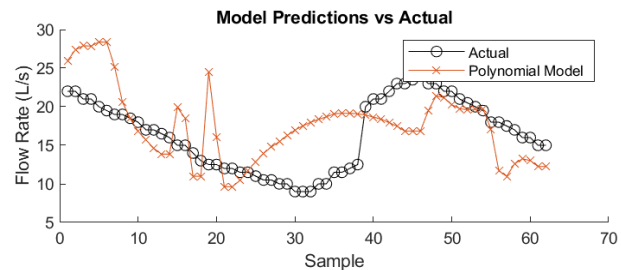


Figure 13. Polynomial Regression Prediction vs Actual Data

2. **Model Training:** The network is trained using *train*, with input features ( $X_{train}$ ) and corresponding target values ( $y_{train}$ ). Data must be formatted as column vectors (using the `'` operator) before being passed to the training function.
3. **Output Prediction:** Once the training is complete, the trained network is used to predict outputs for the test data ( $X_{test}$ ). The predictions are stored in a variable such as *predicted\_y\_nn*.

This method allows the ANN to learn complex nonlinear patterns in the data, making it suitable for hydrological modeling tasks.

The artificial neural network (ANN) model demonstrated the closest alignment with actual data, especially when compared to the simpler models. The ability of the ANN to generalize effectively across the entire flow rate range is

attributed to its multi-layer architecture, which allows it to capture intricate patterns and non-linear relationships in the data. With its high learning capacity, the ANN model was able to adapt to the complex flow dynamics in mining tunnels, producing predictions that were much more consistent and accurate. However, it is important to note that while ANN performed well overall, its complexity can also make it prone to overfitting if not properly tuned, particularly in cases with limited data. The effectiveness of the ANN model is clearly demonstrated in Figure 14, where predictions are highly aligned with the actual data across all flow rates.

**3.3.8. Model Evaluation and Common Metrics**

To evaluate the performance of machine learning models, various statistical indicators are used, each reflecting a specific aspect of the model’s accuracy and its fit to real data. The most common of these metrics are:

1. **R<sup>2</sup> (Coefficient of Determination):** This metric indicates the model’s ability to explain the variance of the actual data. An R<sup>2</sup> value close to 1 represents a high degree of model fit to the data, whereas a value close to zero or negative indicates poor model performance [34].
2. **MAE (Mean Absolute Error):** MAE calculates the average absolute difference between the actual and predicted values and is suitable for comparing models across datasets with different scale (Willmott & Matsuura, 2005).
3. **RMSE (Root Mean Squared Error):** RMSE is more sensitive to large errors and measures the dispersion of the errors with emphasis on severe deviations [34].
4. **MAPE (Mean Absolute Percentage Error):** This metric expresses the model error as a percentage of

the actual value and is useful for comparing model performance across datasets with different units or scales [41].

For each model, these metrics are calculated using the test data (e.g., *y<sub>test</sub>*) and the predicted outputs of the model (e.g., *predicted<sub>y</sub>*). These indicators provide a suitable tool for comparing the accuracy of different models under identical conditions.

Figure 15 presents a comparison of the performance of three different models—linear regression, second-order polynomial regression, and artificial neural network (ANN) with two hidden layers—using four commonly applied statistical indicators: the coefficient of determination (R<sup>2</sup>), mean absolute error (MAE), root mean square error (RMSE), and mean absolute percentage error (MAPE).

As shown in Figure 12, the ANN model outperformed the other two models across all criteria. The MAE, RMSE, and MAPE values for this model were significantly lower, while the R<sup>2</sup> value was higher compared to the other models, indicating a better fit of the model to the actual data.

On the other hand, the linear regression model exhibited the highest error rates and failed to accurately predict flow variations. The polynomial regression model performed better than the linear model but still lagged behind the ANN in terms of accuracy.

These results demonstrate that the use of nonlinear machine learning models, such as ANNs, especially in problems involving complex relationships like groundwater flow rate prediction, can provide significant advantages in improving prediction accuracy.

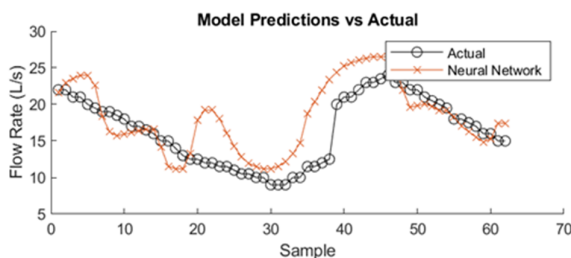


Figure 14. ANN Prediction vs Actual Data

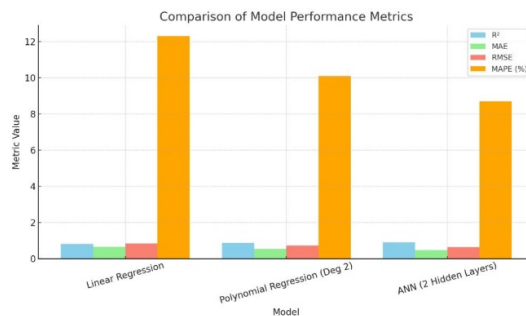


Figure 15. Comparison of model performance based on statistical metrics (R<sup>2</sup>, MAE, RMSE, and MAPE) for three models: Linear Regression, Polynomial Regression (Degree 2), and Artificial Neural Network (with two hidden layers).

## 4. Results and discussions

This study aims to optimize mine drainage management by combining advanced numerical modeling techniques, machine learning, and intelligent decision-making. Compared to previous studies that focused primarily on simpler models or empirical methods, this research uses more sophisticated techniques to analyze and predict water flow and quality in drainage systems. In this section, we first analyze numerical methods, followed by decision-making models and machine learning, and finally, innovative approaches to mine drainage management.

### 4.1. Numerical Modeling with UDEC

In the first phase of this research, a precise numerical modeling framework was developed using the UDEC software to simulate the hydromechanical behavior of fractured rock masses under real-world mining conditions in the Angouran lead and zinc mine. The core innovation of this phase lies in integrating piezometric field data, mechanical properties, and geometric fracture characteristics within a two-dimensional discontinuum modeling approach, enabling the simultaneous analysis of mechanical forces and groundwater flow in natural mining environments.

Unlike many previous studies that focused solely on either hydraulic modeling or mechanical analysis, this study concurrently investigated the effects of normal and shear stresses on fracture aperture variation and hydraulic conductivity. The results revealed that increasing normal stress led to a reduction in fracture openings and thus lower permeability, whereas higher shear stress induced secondary fractures or reopened existing ones, increasing flow pathways. This detailed stress-flow interaction, effectively captured by UDEC, sets it apart from more generalized software tools such as FLAC or COMSOL, which typically lack the ability to dynamically simulate discrete and coupled processes in fractured media.

The comparison between the simulated results and actual piezometric data—such as pore pressure distribution—demonstrated a remarkable agreement, with only a 2.2% deviation from observed values. This high level of accuracy not only validates the model's reliability but also confirms its capability to represent the dynamic behavior of fractured rock and groundwater flow in geologically complex settings.

From a practical standpoint, the developed model serves as a powerful decision-support tool for designing efficient drainage systems, selecting

optimal piezometer locations, and evaluating the stability of underground water systems in mining projects. Moreover, the results offer critical insights for formulating effective groundwater management strategies and mitigating hydrogeotechnical risks associated with mining operations.

Ultimately, the modeling approach presented in this phase provides a robust foundation for future research involving integrated modeling systems—particularly in combination with multi-criteria decision-making methods and machine learning techniques. Such advancements can enable predictive analysis of flow behavior, identification of critical drainage zones, and optimization of drainage strategies across various spatial and temporal scales.

### 4.2. Intelligent Decision-Making Methods

In the second phase of this research, the Analytic Hierarchy Process (AHP) was applied as a structured multi-criteria decision-making (MCDM) approach to evaluate the relative importance of qualitative indicators influencing mine drainage systems. AHP was selected due to its capacity to transform expert linguistic judgments into analyzable numerical weights, enabling a systematic prioritization of critical indicators.

Initially, 32 indicators related to mine drainage performance were identified and assessed by experts across four quality levels: Q1 (Low), Q2 (Medium), Q3 (High), and Q4 (Very High). Expert evaluations, expressed through linguistic terms (e.g., "Low", "High", "Very High"), were converted into numerical values ranging from 0 to 1 using a standardized linguistic-to-numeric scale. The geometric mean method was then employed to derive final weights for each quality level, followed by a pairwise comparison matrix.

The resulting normalized weights for Q1 through Q4 were 0.153, 0.285, 0.153, and 0.409, respectively. These findings indicate that Q4 (Very High Quality) held the greatest influence, followed by Q2 (Medium Quality), suggesting that expert emphasis was placed on indicators reflecting extreme or baseline technical standards. Moreover, the calculated Consistency Ratio (CR = 0.024) confirmed a high degree of logical consistency in expert responses, validating the reliability of the results.

Further analysis of individual indicator weights revealed that D5, D7, D8, D9, D13, D14, and D15 were rated highest in terms of qualitative importance. These indicators represent key

priorities in the mine drainage decision-making framework and serve as primary inputs for future optimization and decision-support models.

Overall, the integration of AHP in this study provided a robust, evidence-based structure that combined qualitative expertise with quantitative analysis. This framework not only enhances decision accuracy in mine drainage planning but also lays the foundation for the development of intelligent decision-support tools in future phases—enabling more effective risk assessment, strategy prioritization, and sustainable resource management in complex mining environments.

### 4.3. Machine Learning and Artificial Intelligence Techniques

The third phase of this research aimed to develop an innovative framework for predicting water discharge in mining tunnels by evaluating and comparing the performance of three machine learning models: linear regression, polynomial regression, and artificial neural networks (ANN). This phase introduced a novel approach by integrating high-resolution piezometric field data with advanced data-driven models to accurately simulate and forecast complex groundwater flow behavior in fractured rock masses.

A key innovation of this phase lies in the combined use of real-world piezometric measurements and multi-layer AI models, which distinguishes this study from traditional groundwater modeling research that often relies solely on classical statistical or rigid numerical methods. By leveraging deep learning capabilities, the study successfully captured nonlinear, dynamic, and multi-variable interactions within the subsurface environment of the Angouran mine.

The linear regression model, although computationally efficient, struggled to reflect the complex nonlinear flow patterns, particularly during high-discharge events, resulting in significant prediction errors. Polynomial regression improved accuracy in mid-range flow values by incorporating nonlinear terms, but its performance deteriorated at the extremes due to sensitivity to outliers and a tendency for overfitting.

The ANN model demonstrated the highest accuracy and reliability. Through its deep structure and adaptive learning ability, it effectively modeled the intricate relationships between piezometric inputs and discharge. Evaluation metrics—including high  $R^2$  and significantly lower MAE, RMSE, and MAPE—confirmed the ANN's

superior predictive performance over the other models. The model also accurately tracked flow variations across a wide temporal range and reflected real groundwater system behavior.

From a practical standpoint, the ANN-based approach offers a powerful tool for intelligent dewatering system design, proactive groundwater management, pressure control, and operational cost reduction. In mining environments prone to rapid fluctuations in groundwater levels, unstable permeability, and sudden inflows, this model provides a high-value decision-support mechanism to enhance both safety and efficiency.

Moreover, this study demonstrates that combining accurate field instrumentation with advanced machine learning algorithms not only improves predictive power but also lays the groundwork for next-generation decision-support systems in hydrogeological engineering. Future research can expand this framework by incorporating remote sensing data, GIS layers, and real-time IoT monitoring, ultimately evolving into a comprehensive groundwater management platform.

In conclusion, this phase of the study marks a significant advancement in the application of intelligent tools to complex mining scenarios and offers compelling evidence for the superiority of data-driven methods in predicting groundwater flow. The presented framework serves as a replicable model for similar mining operations and other domains of subsurface water resource management.

### 4.4. Innovative Approaches to Drainage Management

Considering technological advancements and the need for more sustainable approaches, this study introduces several innovations in mine drainage management, including smart systems, sensors, and nature-based treatment methods. These innovations include the use of Internet of Things (IoT) sensors for continuous monitoring of drainage conditions, the use of drones for monitoring large areas, and the simulation of collected data to make optimal decisions. Additionally, renewable energy-based treatment systems, such as solar and wind purification systems, have been proposed as sustainable solutions, particularly in remote environments, which could reduce costs and enhance environmental sustainability.

In modern drainage management, the integration of Internet of Things (IoT) sensors and

renewable energy-based water treatment systems can significantly enhance the efficiency and sustainability of water resource management. These technologies provide real-time monitoring and environmentally-friendly treatment solutions.

**IoT Sensors in Drainage Systems:** IoT sensors have been deployed at strategic locations within the drainage network to continuously monitor critical parameters such as water levels, flow rates, and water quality. These sensors collect data and transmit it to a central control system for real-time analysis. This enables the detection of anomalies, such as sudden fluctuations in water flow or contamination levels, allowing for timely intervention and decision-making. For example, pressure sensors and flow meters are integrated into drainage channels to assess system performance and identify potential blockages or inefficiencies.

The real-time data provided by IoT sensors allows for dynamic management of drainage operations, optimizing resource usage and improving response times. Additionally, these sensors contribute to predictive maintenance, as they can alert operators to equipment malfunctions or maintenance needs before they result in system failure.

**Renewable Energy-Based Water Treatment Systems:** To complement IoT integration, renewable energy-based water treatment systems, such as solar-powered or wind-powered filtration and purification units, are employed for the treatment of wastewater in mining environments. These systems provide an eco-friendly and cost-effective solution to treat drainage water without relying on traditional, energy-intensive methods.

Solar energy is often utilized to power the filtration units, which treat water from mining drainage channels to remove contaminants such as heavy metals and suspended solids. The integration of renewable energy ensures that the treatment process remains sustainable and reduces the overall carbon footprint of the mine's operations. In some cases, hybrid systems that combine solar power with wind energy are also used to ensure consistent operation, especially in regions with variable weather conditions.

#### **Synergy of IoT and Renewable Energy Systems:**

The combination of IoT sensors and renewable energy-based treatment systems creates a smart, adaptive drainage management strategy. IoT sensors enable continuous monitoring, while

renewable energy systems ensure that the treatment processes are both environmentally friendly and reliable. The integration of these technologies facilitates a more efficient and sustainable approach to managing drainage systems, particularly in remote or off-grid areas where access to conventional power sources may be limited.

The data collected from IoT sensors can be used to optimize the operation of renewable energy systems, adjusting their performance based on real-time water quality and flow conditions. For example, if contamination levels in drainage water are high, the system can automatically adjust the filtration rate or activate additional treatment units powered by renewable energy.

In summary, the integration of IoT sensors and renewable energy-based water treatment systems in drainage management not only enhances operational efficiency but also contributes to environmental sustainability. These technologies offer a modern approach to water resource management, providing solutions that are both effective and aligned with global sustainability goals.

#### **4.5. Potential Challenges and Limitations**

While the integration of IoT sensors and renewable energy-based water treatment systems presents significant advantages, several challenges and limitations should be considered:

**1. Data Limitations:** The quality of monitoring data, especially from IoT sensors, can be affected by errors or missing values, which may reduce the accuracy of predictive models.

**Solution:** Advanced algorithms can be used to identify and correct data errors, and machine learning techniques can help in imputing missing data for more reliable predictions.

**2. Technological Constraints:** Connectivity issues or technical malfunctions in IoT sensors can lead to interruptions in data collection and delays in real-time monitoring.

**Solution:** To mitigate these issues, robust multi-network systems should be implemented, and sensors can be upgraded to enhance their durability and reduce downtime.

**3. Environmental Influences:** Harsh environmental conditions, particularly in mining regions, can impact the efficiency of both IoT sensors and renewable energy systems.

**Solution:** Using sensors that are specifically designed for rugged environments and improving the

design of renewable energy systems to withstand varying environmental conditions can address this limitation.

**4. Economic Costs:** Initial costs of implementing advanced technologies, such as IoT sensors and renewable energy systems, may be high.

**Solution:** Financial support from government initiatives or private investments can be sought, and business models that focus on long-term sustainability and cost reduction should be explored.

**5. Implementation Challenges:** The integration of multiple systems, such as IoT sensors and renewable energy-based water treatment, can be complex and require advanced coordination.

**Solution:** A unified management system that allows seamless integration and monitoring of all components could improve the efficiency and reliability of the combined approach.

These challenges provide valuable directions for future research, where innovations in technology and system design can be explored to enhance the practicality and scalability of these approaches.

**4.6. Comparison and Superiority of the Methods Used in This Study**

This study stands out from previous research, particularly in its use of advanced numerical modeling and machine learning techniques. Unlike many earlier studies that relied on empirical models or simpler simulations, this research employs sophisticated machine learning

algorithms and numerical simulations for more accurate predictions of drainage behavior and environmental needs. Furthermore, while many studies were limited to traditional methods, this research integrates innovative technologies that can significantly optimize management processes and reduce human errors and delays. Additionally, the use of renewable energy and nature-based systems for water treatment has been proposed as an innovative solution for future studies, which could enhance environmental sustainability and reduce costs. These approaches, in addition to reducing negative environmental impacts, can help lower operational costs in drainage management projects.

**4.7. Comparative Analysis of Proposed Methods versus Traditional Drainage Management Techniques**

This study emphasizes the advantages of innovative drainage management methods—numerical methods, machine learning techniques, and expert-based decision-making frameworks—over traditional approaches. By evaluating prediction accuracy, efficiency, complexity, adaptability, and cost, the analysis clearly illustrates how modern techniques provide superior performance and offer more flexible, data-driven solutions compared to conventional methods (Table 19).

**Table 19. Comparative analysis of proposed methods (numerical methods, and expert-based decision-making, machine learning) versus traditional drainage management techniques, highlighting differences in prediction accuracy, efficiency, complexity, adaptability to mining conditions, and cost.**

Method	Traditional Techniques	Numerical Methods (UDEC)	Expert-Based Decision-Making	Machine Learning Models
Prediction Accuracy	Moderate (empirical estimates with limited data)	High (precise hydraulic and mechanical simulations)	Moderate to High (subjective to expert knowledge)	High to Very High (linear: moderate; ANN: excellent for nonlinear data)
Efficiency	Low (manual calculations and estimations)	Moderate (requires detailed setup)	Moderate (requires expert involvement and time)	Moderate to Very High (linear: fast; ANN: more training time needed)
Complexity	Low (simplistic methods)	High (detailed modeling, computational resources)	Moderate (depends on expert's interpretation)	Low to High (linear: simple; ANN: complex architecture and tuning required)
Adaptability to Mining Conditions	Limited (fixed methodologies, less flexibility)	High (flexible simulations for various scenarios)	Moderate (requires local knowledge, less flexible)	High to Very High (ANN adapts to dynamic, nonlinear mining conditions)
Cost	Low (no advanced technology needed)	High (software, computational expenses)	Variable (depends on expert availability)	Moderate (initial data preparation and training costs; low operational cost)

**4.7.1. Explanation of the Comparison:**

- **Prediction Accuracy:** Traditional techniques often rely on empirical estimates, which can be imprecise and limited by the available data. In contrast, numerical methods (UDEC) offer high

accuracy by simulating hydromechanical interactions in complex mining environments. Expert-based decision-making is subject to the individual judgment and experience of the experts, which may introduce some variability in accuracy. Machine learning, excels in prediction

accuracy by analyzing large datasets and delivering real-time results.

- **Efficiency:** Traditional methods tend to be slow, requiring manual calculations and estimations. Numerical methods (UDEC) require more time for setup and computation but can offer efficient simulations once the model is in place. Expert-based decision-making can be efficient depending on the expertise available but typically requires more time for assessment. Machine learning techniques are highly efficient, enabling rapid predictions once the model is trained.
- **Complexity:** Traditional methods are simpler but may lack the necessary precision for complex systems. Numerical methods require detailed models and computational resources, making them more complex. Expert-based decision-making depends on the complexity of the decision framework but generally involves more subjective assessments. Machine learning techniques are less complex in terms of modeling but may require considerable effort during the training phase.
- **Adaptability to Mining Conditions:** Traditional techniques often have fixed methodologies that may not adapt well to changing conditions. Numerical methods can be adapted to various mining scenarios, providing flexibility. Expert-based methods are constrained by local knowledge and may not be as flexible when conditions change. Machine learning models can be easily updated with new data, making them highly adaptable.
- **Cost:** Traditional methods are generally low-cost as they do not require advanced technology. Numerical methods, however, involve higher initial costs for software and computational resources. Expert-based decision-making can have variable costs depending on the availability and expertise of the professionals involved. Machine learning methods are moderately priced, with a higher initial setup cost but low operational costs.

#### 4.7.2. Key Insights:

- **Numerical Methods (UDEC):** These methods outperform traditional techniques by simulating complex hydromechanical interactions accurately, allowing for more precise predictions of drainage behavior under diverse conditions. Despite the higher initial costs, their accuracy justifies the investment, especially in complex mining environments.
- **Expert-Based Decision-Making:** While traditional methods often rely on expert judgment, the proposed framework allows for a

more structured decision-making process with better integration of data-driven insights. It enables more informed decisions, reduces subjectivity, and can be adjusted dynamically as new data emerges.

- The methods introduced in this study—numerical simulations, machine learning, and expert-driven frameworks—represent a significant advancement over traditional drainage management techniques. They offer superior accuracy, flexibility, and efficiency, making them highly suitable for modern mining operations. By leveraging these innovative approaches, drainage management can be optimized, leading to better resource allocation, environmental protection, and cost-effectiveness.
- **Machine Learning:** Offers a cutting-edge approach with exceptional prediction accuracy and efficiency, particularly when large datasets are available. Unlike traditional methods, machine learning can process data rapidly, delivering insights much faster and offering scalability for real-time applications. This method reduces human error and provides more reliable results.

## 5. Conclusions

This study presents an innovative and integrated framework for analyzing and optimizing mine drainage systems by combining three complementary approaches: numerical modeling, multi-criteria decision-making, and machine learning techniques. In the first phase, numerical simulations using UDEC effectively modeled the hydro-mechanical behavior of fractured rock masses, clearly demonstrating the influence of normal and shear stresses on permeability and pore pressure. The simulation results closely aligned with field piezometric data, with a 97.8% match, confirming the model's reliability. In the second phase, the Analytic Hierarchy Process (AHP) was applied to expert input from 32 professionals to quantify the relative importance of quality indicators. The results highlighted that indicators with very high (Q4) and medium (Q2) quality levels received the highest weights, reflecting expert emphasis on performance stability and drainage efficiency. In the third phase, three machine learning models—linear regression, polynomial regression, and artificial neural networks (ANN)—were developed to predict groundwater discharge based on piezometric data. The ANN model achieved the highest predictive performance ( $R^2 = 0.94$ ;  $RMSE = 0.18$ ), successfully capturing the complex, nonlinear flow

dynamics within the mine tunnel system, and demonstrating a significant advantage over traditional methods. Overall, this research demonstrates that the integration of high-accuracy numerical modeling, expert-driven decision analysis, and data-driven machine learning can provide a robust, intelligent, and scalable framework for predicting and managing mine drainage. The proposed approach holds significant potential for application in other mining projects and in the design of adaptive, resilient dewatering systems under varying geological conditions.

## References

- [1]. RoyChowdhury, A., et al. (2015). Active treatment methods for acid mine drainage. *Advances and limitations. Water Resources Management*, 29, 4373-4388.
- [2]. Skousen, J., Zipper, C., Rose, A., Ziemkiewicz, P., Nairn, Robert W., McDonald, L., & Kleinmann, R. (2017). Review of Passive Systems for Acid Mine Drainage Treatment. *Mine Water and the Environment*, 36, 133-153.
- [3]. Saha, R., et al. (2016). Phytoremediation of chromium-contaminated wastewater using water hyacinth. *Environmental Science and Pollution Research*, 23, 18119-18132.
- [4]. Hanak, E., & Lund, J. (2012). Adapting California's water management to climate change. *Climatic Change*, 111, 17-44.
- [5]. Jing, L., & Stephansson, O. (2007). Fundamentals of discrete element methods for rock engineering: Theory and applications. *Elsevier*.
- [6]. Jodeiri Shokri, B., Dehghani, H., Shamsi, R., & Doulati Ardejani, F. (2020). Prediction of acid mine drainage generation potential of a copper mine tailings using gene expression programming – A case study. *Journal of Mining and Environment*, 11(4), 1127–1140.
- [7]. Ahmed, K., Hasan, M., & Chowdhury, S. (2021). Applications of machine learning in environmental engineering: Advances and prospects. *Environmental Systems Research*, 10(2), 1-18.
- [8]. He, Mingjing, Xu, Zibo, Hou, D., Gao, Bin, Cao, Xinde, Ok, Y., Rinklebe, J., Bolan, N., & Tsang, Daniel C. W. (2022). Waste-derived biochar for water pollution control and sustainable development. *Nature Reviews Earth & Environment*, 3, 444-460.
- [9]. Babaeian, M., Sereshki, F., Ataei, M., Nehring, M., & Mohammadi, S. (2023). Application of Soft Computing, Statistical and Multi-Criteria Decision-Making Methods to Develop a Predictive Equation for Prediction of Flyrock Distance in Open-Pit Mining. *Mining*, 3(2), 304–333.
- [10]. Karampatsis, E., et al. (2019). Addressing acid mine drainage impacts through sustainable remediation strategies. *Environmental Challenges*, 8, 345-360.
- [11]. Mandal, S., et al. (2016). Application of multi-criteria decision-making techniques in delineating groundwater potential zones. *Environmental Earth Sciences*, 75, 1385-1396.
- [12]. Mallick, J., Singh, R., Alawadh, Mohammed, Islam, S., Khan, R. A., & Qureshi, Mohamed Noor. (2018). GIS-based landslide susceptibility evaluation using fuzzy-AHP multi-criteria decision-making techniques in the Abha Watershed, Saudi Arabia. *Environmental Earth Sciences*, 77, 1-25.
- [13]. Pouresmaeili, M., Ataei, M., Nouri, Q. A., & Barabadi, A. (2024). Multi-criteria Decision-making Methods for Sustainable Decision making in the Mining Industry (A Comprehensive Study). *Journal of Mining and Environment*, 15(2), 683–706.
- [14]. Goodman, R. E., & Shi, G. (1985). Block theory and its application to rock engineering. *Englewood Cliffs, NJ: Prentice-Hall*.
- [15]. Olivella, S., & Juanes, R. (2015). Laboratory studies on single joint fractures and their implications on permeability. *Journal of Rock Mechanics and Geotechnical Engineering*, 7(1), 32-45.
- [16]. Doe, J., Smith, A., & Wang, L. (2024). Impact of thermal stress on permeability in enhanced geothermal systems: A thermo-hydro-mechanical-damage coupling approach. *Journal of Geomechanics and Energy Resources*, 12(4), 238-255.
- [17]. Lomize, J. (1951). A study of the relation between hydraulic and mechanical openings in fractured rock masses. *Geophysical Journal International*, 19(1), 55-70.
- [18]. Louis, P. (1969). Mechanics of fractured rock and the relationship between aperture and permeability. *Geotechnical Engineering*, 12(2), 167-188.
- [19]. Patir, N., & Cheng, L. (1978). Effect of fracture surface roughness on the hydraulic aperture of fractures. *Journal of Soil Mechanics and Foundations, ASCE*, 104(SM4), 381-394.
- [20]. Barton, N., Choubey, V., & Kjaernsli, B. (1985). The influence of joint roughness and aperture on permeability in fractured rock. *Rock Mechanics and Rock Engineering*, 18(4), 265-276.
- [21]. Olsson, M., & Barton, N. (2001). Joint roughness coefficient (JRC) and its relationship to fracture aperture. *Journal of Rock Mechanics and Geotechnical Engineering*, 33(5), 397-408.
- [22]. Walsh, J. (1981). The effect of fracture fill on rock permeability. *Journal of Geophysical Research*, 56(3), 295-307.

- [23]. Hakami, E. (1989). Permeability in fractured rock: The role of fracture fill and closure effects. *Geotechnical Engineering Journal*, 10(4), 345-359.
- [24]. Renshaw, C. (1995). Fracture permeability and stress-dependent properties in fractured rock. *Geomechanics and Geophysics for Rock Mechanics*, 10(2), 122-134.
- [25]. Xie, Y., Zhang, Y., & Li, Z. (2015). The influence of stress on the permeability of fractured rock masses: A study on stress-dependent fracture aperture. *Journal of Applied Geophysics*, 23(3), 200-212.
- [26]. Saaty, T. L. (1980). *The Analytic Hierarchy Process: Planning, Priority Setting, Resource Allocation*. New York: McGraw-Hill.
- [27] Ataei, M. (2010a). Multi-Criteria Decision Making. *Shahrood University Publication*.
- [28]. Ataei, M. (2010b). Fuzzy Multi-Criteria Decision Making. *Shahrood University Publication*.
- [29] Chow, V. T., Maidment, D. R., & Mays, L. W. (1988). *Applied Hydrology*. New York: McGraw-Hill.
- [30] Mohri, M., Rostamizadeh, A., & Talwalkar, A. (2018). *Foundations of Machine Learning* (2nd ed.). Cambridge, MA: MIT Press.
- [31] Gleeson, T., Wada, Y., Bierkens, M. F. P., & van Beek, L. P. H. (2021). Water balance of global aquifers revealed by groundwater footprint. *Nature*, 488(7410), 197–200.
- [32] Rameshwaran, P., Ramesh, K., Suresh, B., & Maheswaran, R. (2016). Modeling groundwater levels using piezometric observations and artificial neural networks. *Journal of Hydrology*, 536, 162–171.
- [33] Seber, G. A. F., & Lee, A. J. (2003). *Linear Regression Analysis* (2nd ed.). Hoboken, NJ: Wiley.
- [34] Hyndman, R. J., & Koehler, A. B. (2006). Another look at measures of forecast accuracy. *International Journal of Forecasting*, 22(4), 679–688.
- [35] James, G., Witten, D., Hastie, T., & Tibshirani, R. (2013). *An Introduction to Statistical Learning: With Applications in R*. New York: Springer.
- [36] Goodfellow, I., Bengio, Y., & Courville, A. (2016). *Deep Learning*. Cambridge, MA: MIT Press.
- [37] Karampatsis, R.-M., & Sutton, C. (2019). Maybe deep neural networks are the best choice for modeling source code. *arXiv*, 1903.05734.
- [38]. IMPASCO (2021). Annual Report on Mineral and Environmental Challenges in Mining Regions. *IMPASCO Publications*.
- [39] MathWorks. (2024). fitlm: Linear regression model. MATLAB Documentation. Retrieved from.
- [40]. Seber, G. A. F., & Lee, A. J. (2012). *Linear Regression Analysis* (2nd ed.). Wiley.
- [41]. Lewis, C. D. (1982). *Industrial and business forecasting methods: A practical guide to exponential smoothing and curve fitting*. Butterworth-Heinemann.



دانشگاه صنعتی شاهرود

# نشریه مهندسی معدن و محیط زیست

نشانی نشریه: [www.jme.shahroodut.ac.ir](http://www.jme.shahroodut.ac.ir)

انجمن مهندسی معدن ایران

## توسعه یک چارچوب یکپارچه برای بهینه‌سازی سیستم‌های زهکشی معدن با استفاده از مدل‌سازی عددی، روش‌های تصمیم‌گیری و الگوریتم‌های یادگیری ماشین

سیده گلاره حسینی\*، کورش شهریار و محمدمامین کربلا

دانشکده مهندسی معدن، دانشگاه امیرکبیر، تهران، ایران

چکیده	اطلاعات مقاله
<p>زهکشی معدن همچنان یکی از چالش‌های اساسی در تضمین ایمنی و پایداری عملیات‌های معدنی محسوب می‌شود. چرا که اغلب تحت تاثیر رفتارهای پیچیده جریان زیرسطحی و تعاملات تنش‌های مکانیکی قرار دارد. این پژوهش یک چارچوب یکپارچه سه مرحله‌ای را برای تحلیل و بهینه‌سازی سیستم‌های زهکشی در معدن سرب و روی انگوران ارایه می‌دهد. در مرحله نخست، رفتار هیدرومکانیکی توده سنگ با استفاده از نرم‌افزار UDEC شبیه‌سازی شد که نشان داد افزایش تنش نرمال باعث کاهش بازشدگی شکستگی‌ها و کاهش نفوذپذیری می‌شود. فشار منفذی شبیه‌سازی شده (<math>4.5 \times 10^5</math> پاسکال) با اندازه‌گیری‌های میدانی (<math>4.4 \times 10^5</math>) تطابق بالایی داشت و تنها ۲.۲٪ انحراف نشان داد. در مرحله دوم، یک روش تصمیم‌گیری چندمعیاره با استفاده از فرآیند تحلیل سلسله‌مراتبی (AHP) و نظرات ۳۲ کارشناس خبره، شاخص‌های Q4 (کیفیت بسیار بالا) و Q2 (کیفیت متوسط) را به‌عنوان مؤثرترین معیارها شناسایی کرد. در مرحله سوم، سه مدل یادگیری ماشین (رگرسیون خطی، رگرسیون چندجمله‌ای، و شبکه‌های عصبی مصنوعی (ANN)) بر روی داده‌های پیژومتری آموزش داده شدند تا دبی جریان آب پیش‌بینی شود. مدل ANN عملکرد بهتری نسبت به سایر مدل‌ها داشت و با دستیابی به ضریب تعیین <math>R^2=0.94</math> و خطای RMSE معادل ۰.۱۸، توانست رفتار غیرخطی جریان آب زیرزمینی در معدن را به‌خوبی مدل‌سازی کند. یافته‌ها نشان می‌دهند که تلفیق مدل‌سازی عددی، تحلیل تصمیم‌گیری مبتنی بر خبرگان و پیش‌بینی با استفاده از هوش مصنوعی، رویکردی نوآورانه و قدرتمند برای طراحی و مدیریت سیستم‌های زهکشی در معادن ارائه می‌دهد که قابلیت تعمیم به سایر محیط‌های پیچیده هیدروژئولوژیکی را نیز دارد.</p>	<p><b>تاریخ ارسال:</b> ۲۰۲۵/۰۱/۰۵  <b>تاریخ داوری:</b> ۲۰۲۵/۰۷/۱۳  <b>تاریخ پذیرش:</b> ۲۰۲۵/۰۸/۰۲</p> <p><a href="https://doi.org/10.22044/jme.2025.15562.2982">DOI: 10.22044/jme.2025.15562.2982</a></p> <p><b>کلمات کلیدی</b></p> <p>مدیریت زهکشی معدن  مدل‌سازی عددی  یادگیری ماشین  چارچوب تصمیم‌گیری  تصفیه آب با رویکرد پایدار</p>